

1 **Pericyte-mediated constriction of renal capillaries evokes no-reflow and kidney injury following**
2 **ischemia**

3 Felipe Freitas and David Attwell

4

5 Department of Neuroscience, Physiology & Pharmacology

6 Andrew Huxley Building

7 University College London

8 Gower Street, London, WC1E 6BT, UK

9

10 **Running title: Pericytes mediate post-ischemic renal no-reflow**

11

12 **Address correspondence to:**

13 David Attwell

14 Email: d.attwell@ucl.ac.uk

15 Tel (+44)-20-7679-7342

16 Department of Neuroscience, Physiology & Pharmacology

17 Andrew Huxley Building

18 University College London

19 Gower Street, London, WC1E 6BT, UK

20 **Keywords:** Renal ischemia; no-reflow; pericytes; kidney injury; descending vasa recta; peritubular
21 capillaries.

1 **Abstract**

2 Acute kidney injury is common, with ~13 million cases and 1.7 million deaths/year worldwide. A
3 major cause is renal ischemia, typically following cardiac surgery, renal transplant or severe
4 hemorrhage. We examined the cause of the sustained reduction in renal blood flow (“no-reflow”),
5 which exacerbates kidney injury even after an initial cause of compromised blood supply is removed.
6 After 60 min kidney ischemia and 30-60 min reperfusion, renal blood flow remained reduced,
7 especially in the medulla, and kidney tubule damage was detected as Kim-1 expression. Constriction
8 of the medullary descending vasa recta and cortical peritubular capillaries occurred near pericyte
9 somata, and led to capillary blockages, yet glomerular arterioles and perfusion were unaffected,
10 implying that the long-lasting decrease of renal blood flow contributing to kidney damage was
11 generated by pericytes. Blocking Rho kinase to decrease pericyte contractility from the start of
12 reperfusion increased the post-ischemic diameter of the descending vasa recta capillaries at pericytes,
13 reduced the percentage of capillaries that remained blocked, increased medullary blood flow and
14 reduced kidney injury. Thus, post-ischemic renal no-reflow, contributing to acute kidney injury,
15 reflects pericytes constricting the descending vasa recta and peritubular capillaries. Pericytes are
16 therefore an important therapeutic target for treating acute kidney injury.

1 **Introduction**

2 The global burden of acute kidney injury is approximately 13 million cases a year (Ponce &
3 Balbi, 2016). It is associated with a high mortality (1.7 million deaths per year, worldwide) (Gameiro
4 et al., 2018; Hoste et al., 2018; Mehta et al., 2016), and COVID-19 has added to its incidence (Ronco
5 et al., 2020). Renal ischemia followed by reperfusion, which can occur after cardiac surgery, renal
6 transplant or severe hemorrhage, is the most common cause of acute kidney injury (Lameire et al.,
7 2006; Lameire & Vanholder, 2001). Sustained renal blood flow reductions occur after ischemia and
8 reperfusion, both in experimental studies and in patients after kidney transplantation (Cristol et al.,
9 1996; Nijveldt et al., 2001; Ramaswamy et al., 2002). Following short periods of ischemia, blood flow
10 to the renal cortex largely recovers following reperfusion, but medullary blood flow remains reduced
11 for a prolonged period, especially in the hypoxia-sensitive outer medulla. Medullary no-reflow is a
12 critical event for amplifying renal tissue injury following reperfusion (Conesa et al., 2001; Olof et al.,
13 1991; Regner et al., 2009).

14 Renal no-reflow has been attributed to various causes, including impaired erythrocyte
15 movement and leukocyte accumulation in renal capillaries, as well as increased intratubular pressure
16 (Bonventre & Weinberg, 2003; Sutton et al., 2002; Wei et al., 2017; Yamamoto et al., 2002).
17 However, after years of investigation, no effective treatment is available, even though no-reflow
18 predicts a worse prognosis after kidney ischemia. We therefore investigated an alternative possible
19 cause of no-reflow, i.e. ischemia-evoked contraction of pericytes that regulate capillary diameter,
20 which might reduce renal blood flow and physically trap red blood cells. Indeed, in the brain and heart
21 contractile pericytes on capillaries play a key role in reducing blood flow after ischemia (Hall et al.,
22 2014; O'Farrell et al., 2017; Yemisci et al., 2009) because capillaries remain constricted by pericytes
23 even when blood flow is restored to upstream arterioles. In the kidney, pericytes are associated with
24 the cortical and medullary peritubular capillaries and the descending vasa recta. They play a key role
25 in regulating renal medullary blood flow (Crawford et al., 2012; Pallone & Silldorff, 2001) which is a
26 crucial variable for meeting the contradictory demands of preserving cortico-medullary osmotic
27 gradients to allow water retention in the body, while maintaining adequate oxygen and nutrient

1 delivery. This raises the question of whether pericytes also play a role in generating renal no-reflow
2 after ischemia.

3 Few studies have investigated how ischemia affects renal pericytes (Kwon et al., 2008;
4 McCurley et al., 2017; Zhang et al., 2018), and whether pericytes contribute to renal no-reflow.
5 However, peritubular pericytes are damaged in cortical tissue of cadaveric renal allografts following
6 ischemia-reperfusion (Kwon et al., 2008), suggesting that renal blood flow control may be disrupted
7 after ischemia by pericyte dysfunction. Here we show that pericyte-mediated capillary constriction,
8 especially of the descending vasa recta, makes a crucial contribution to no-reflow following renal
9 ischemia and reperfusion. We further show that targeting pericyte-mediated constriction
10 pharmacologically can reduce ischemia-evoked acute kidney injury.

11 **Results**

12 **No-reflow after renal ischemia and reperfusion**

13 We used a combination of laser Doppler perfusion measurements, low magnification imaging
14 of blood volume, and high magnification imaging that resolved individual capillaries, to assess the
15 magnitude and cause of changes of renal perfusion after ischemia. Ischemia for 1 hour decreased
16 perfusion of the renal medulla and cortex by ~90% (both $p < 0.0001$ vs. control; assessed with laser
17 Doppler: Figure 1a ,b). After 30 min reperfusion, blood flow recovered to 49% of control
18 (significantly reduced, $P = 0.005$, Figure 1a) in the medulla, but to 75% in the cortex ($P=0.047$,
19 Figure 1b) (Regner et al., 2009). Perfusion was stable in the contralateral kidney throughout (Figure
20 1a, b). After 60 min reperfusion, medullary perfusion remained compromised at 40% of the control
21 level ($P=0.017$, Figure S1), but cortical perfusion had fully recovered (to ~20% above the control
22 value, not significant, $P=0.092$, Figure S1). Despite this flow recovery, we show below that
23 peritubular capillaries in the cortex can become blocked after ischemia.

24 After ischemia and reperfusion *in vivo*, assessing the volume of perfused vessels in fixed
25 kidney slices, as the summed FITC-albumin intensity over ROIs, also demonstrated that renal
26 ischemia and reperfusion led to no-reflow in the medulla compared with the non-ischemic kidney's
27 medulla (the perfusing blood volume was reduced by ~50%, $P=0.002$; Figure 1c, d, f). Microscopic

1 analysis resolving individual capillaries showed that this blood volume reduction was associated with
2 a large reduction in capillary perfusion (Figure 2). The total perfused capillary length in 100 μm deep
3 confocal z-stacks (frame size 640.17x 640.17 μm) was reduced by 35% (contralateral control
4 14689 \pm 3477 μm vs. ischemia 9527 \pm 1183 μm , $P=0.038$), the number of perfused capillary segments
5 was reduced by 54% (control 530 \pm 82 vs. ischemia 244 \pm 30, $P=0.03$), and the overall perfused
6 microvascular volume fraction was reduced by 51% (control 0.116 \pm 0.006 vs. ischemia 0.057 \pm 0.006,
7 $P=0.003$; Figure 2e-g).

8 In the cortex, perfusion was reduced less than in the medulla after ischemia and reperfusion,
9 i.e. by 23.5% compared with non-ischemic kidneys ($P=0.0075$, Figure 1c, d, g). Furthermore,
10 although a small percentage of afferent and efferent arterioles, and glomeruli, were not perfused in
11 control conditions, this percentage did not increase significantly after ischemia (Figure 3a, b, g), and
12 the arterioles' diameter was not reduced compared with those in non-ischemic kidneys (Figure 3a, b,
13 h, i). Similarly, it has been reported that upstream arteries are not constricted after ischemia
14 (Yamamoto et al., 2002). In contrast, the total perfused peritubular capillary length in the 100 μm
15 deep z-stacks (control 16441 \pm 1577 μm vs. ischemia 5411 \pm 2735 μm , reduced by 67%, $P=0.03$), the
16 number of perfused capillary segments (control 550 \pm 32 μm vs. ischemia 349 \pm 54, reduced by 36.5%,
17 $P=0.01$) and the overall perfused peritubular capillary volume fraction (control 0.12 \pm 0.01 vs.
18 ischemia 0.06 \pm 0.02, reduced by 50%, $P=0.01$) were greatly reduced in the cortex when compared
19 with non-ischemic kidneys (Figure 3d-f). Thus, the effect of ischemia and reperfusion is
20 predominantly on the microvasculature, i.e. the peritubular cortical capillaries and the vasa recta,
21 rather than on arteriolar segments of the kidney circulation. The Rho kinase data shown in Fig. 3 are
22 discussed below.

23 **Pericytes constrict descending vasa recta after ischemia and reperfusion**

24 Higher magnification images demonstrated that, in control kidneys, only 9.7% of the
25 descending vasa recta (DVR) capillaries were blocked (Figures 2b, 4d), i.e. were not perfused by
26 FITC-albumin (Figures 2c, 4a-d). However, after ischemia and 30 mins reperfusion, 78% of the DVR
27 capillaries were blocked (Figures 2c, 4a-d). Some capillaries were fully perfused and some completely

1 unperfused throughout the area assessed, whereas some exhibited an abrupt cessation of blood flow
2 with a decrease of FITC-albumin intensity over a few microns (Figures 2c, 4a-c). At block sites, the
3 diameter of the FITC-albumin luminal labeling at the final position blood reached was significantly
4 lower in ischemic DVR capillaries compared with that at the much smaller number of block sites in
5 non-ischemic controls (control $6.5\pm 0.3\ \mu\text{m}$ vs. ischemia $3.5\pm 0.4\ \mu\text{m}$; $P=0.039$, Figure 4e). Thus, an
6 ischemia-induced constriction of the DVR promotes blockage, which persists even after reperfusion.

7 Erythrocyte protein glycoprotein A was labelled to assess if red blood cells were trapped at
8 capillary regions of reduced diameter. Red blood cells were associated with only a small percentage
9 of blockage sites in ischemic kidneys (5.8% of 85 blockages in 137 vessels from 2 animals), and even
10 where red blood cells were near the capillary blockages they did not always block blood flow because
11 FITC-albumin could pass the red blood cells (Figure S2a, b).

12 In the brain (Hall et al., 2014; Yemisci et al., 2009) and heart (O'Farrell et al., 2017) post-
13 ischemic capillary constriction reflects pericyte contraction, which occurs near pericyte somata where
14 circumferential processes originate (Nortley et al., 2019). From NG2 labelling we observed that many
15 DVR blockages were close to pericyte somata, or near to pericyte circumferential processes connected
16 to the soma (Figure 4b-c), suggesting that contraction of these juxta-somatic processes evoked
17 capillary block. We measured the distance of 27 blockages to the nearest pericyte soma. The
18 probability distribution of this distance is compared with that of the inter-pericyte distance in Figure
19 4f (if blocks did not depend on pericytes, the probability distribution of the blockage-pericyte distance
20 would be constant until half the distance between pericytes). The mean blockage-pericyte distance
21 was $4.87\pm 0.33\ \mu\text{m}$ after ischemia and reperfusion, which is less than a quarter of the distance between
22 DVR pericytes ($22.85\pm 0.93\ \mu\text{m}$, from 118 pericyte pairs). Thus, these data are consistent with
23 pericyte constriction generating the DVR blockages.

24 In control conditions, the few blockages occurring were mainly in regions where the inter-
25 pericyte distance was larger. The mean distance from a blockage to the nearest pericyte soma was also
26 larger ($14.98\pm 1.36\ \mu\text{m}$, $p<0.0001$ compared to post-ischemia), suggesting a different block
27 mechanism in control conditions.

1 To assess pericyte-mediated DVR constriction further, we measured the FITC-albumin
2 labelled lumen diameter at 5 micron intervals upstream of pericyte somata (upstream so there was
3 FITC-albumin in the vessel: Figure 4g). After ischemia and reperfusion, the diameter was
4 significantly reduced (by 41%, $p=0.0001$) near the pericyte somata compared with non-ischemic
5 kidneys, but less reduced further from the somata. The diameter significantly increased with distance
6 from the somata after ischemia and reperfusion ($P=0.039$ comparing the slope of the best-fit ischemia
7 regression line with zero) but not in control conditions ($P=0.084$), implying constriction preferentially
8 near the pericyte somata (Figure 4g) and identifying pericytes as the origin of the diameter reduction.
9 Such constrictions will reduce blood flow directly by increasing the vascular resistance, and may also
10 lead to blood cells becoming trapped at the regions of narrowed diameter, thus occluding the vessel
11 and further reducing blood flow.

12 We assessed whether the endothelial glycocalyx (eGCX) contributed to DVR blockages.
13 Labelling showed that eGCX is fairly uniformly present along capillaries, and this was not altered
14 after ischemia (Figure S2f-g). There was no correlation between eGCX intensity and capillary
15 diameter in control or ischemic conditions (Figure S2h). Thus, eGCX is not particularly associated
16 with pericytes (Figure S2f), so the co-location of diameter reduction and blockages with pericyte
17 somata presumably reflects pericyte process contraction rather than obstruction by eGCX.

18 **Pericytes constrict peritubular cortical capillaries *in vivo* after ischemia and reperfusion**

19 Two-photon microscopy *in vivo*, of mice expressing dsRed in pericytes, revealed peritubular
20 cortical pericytes constricting and blocking capillaries after ischemia and reperfusion (Figure 5a-c).
21 This reduced the mean capillary diameter (averaged over all positions measured) from 10.8 ± 0.2 to
22 8.1 ± 0.5 μm ($p<0.0001$). To quantify whether ischemia-evoked blockages occurred disproportionately
23 close to pericytes, we measured the distance of 15 blockages to the nearest pericyte soma. This
24 distance was 4.12 ± 0.39 μm , which is only 10% of the mean distance between peritubular cortical
25 pericytes (41.3 ± 2.6 μm , from 103 pericyte pairs). A plot of capillary diameter versus distance from
26 pericyte somata (Figure 5d) showed that ischemia and reperfusion reduced the diameter by 40% at the
27 somata (control 11.2 ± 0.5 vs. ischemia 6.76 ± 1.05 μm , $P=0.001$) with no significant effect on diameter

1 far from the somata (control $10.3 \pm 0.2 \mu\text{m}$ vs. ischemia $9.6 \pm 0.5 \mu\text{m}$, $P=0.115$). As in the medulla, the
2 diameter increased significantly with distance from the pericyte somata after ischemia ($P=0.046$
3 comparing the slope of the best-fit regression line with zero) while in control conditions it did not
4 (diameter decreased insignificantly with distance, $P=0.10$). Thus, capillaries are constricted
5 specifically near cortical pericytes.

6 **Rho kinase inhibition reduces pericyte constriction and no-reflow**

7 The contractility of pericytes depends partly on Rho kinase activity (Durham et al., 2014;
8 Hirunpattarasilp et al., 2019; Homma et al., 2014; Kutcher et al., 2007). The Rho kinase inhibitor,
9 hydroxyfasudil (3 mg/kg; i.v.), applied at the time of reperfusion to mimic a possible therapeutic
10 intervention, significantly inhibited the decrease of renal medullary perfusion seen after ischemia-
11 reperfusion (Figure 1a, e-f). *In vivo*, blood flow in the medulla (after 30 mins reperfusion) was
12 increased 3.8-fold compared to ischemia without hydroxyfasudil ($P=0.002$, Figure 1a).
13 Hydroxyfasudil induced a faster recovery of medullary blood flow than BQ123 (0.5 mg/kg, i.v.), an
14 endothelin-A receptor antagonist (Figure S1c), but both resulted in blood flow at 30 mins reperfusion
15 that was not significantly different from the control value ($P=0.8$ and 0.38 respectively) and was
16 significantly higher than the flow seen after ischemia without either drug ($P=0.01$ for both drugs). In
17 contrast, the angiotensin II type 1 (AT1) receptor antagonist valsartan (1 mg/kg i.v.) speeded the
18 initial post-ischemic recovery of medullary blood flow, but did not return it to baseline by 30 mins
19 reperfusion (Figure S1c). In the cortex, blood flow recovery on reperfusion was speeded by
20 hydroxyfasudil and, after 30 mins of reperfusion, was increased 1.48-fold compared to ischemia alone
21 ($P=0.02$, Figure 1b). These data suggest that, in the medulla especially, activation of Rho kinase (in
22 part downstream of ischemia-evoked activation of endothelin A receptors (Prakash et al., 2008;
23 Wilhelm et al., 1999; Yamamoto et al., 2000)) contributes to ischemia-evoked pericyte-mediated
24 capillary constriction.

25 Renal perfusion with post-ischemic inhibition of Rho kinase was also assessed in slices of
26 fixed kidney (see above). Treatment with hydroxyfasudil during post-ischemic reperfusion prevented
27 medullary no-reflow after ischemia and reperfusion: the blood volume was increased 2.3-fold

1 compared to ischemia alone ($P=0.003$, Figure 1e-f), so that it did not differ significantly from that in
2 control kidney ($P=0.47$). Hydroxyfasudil also increased ~ 2.9 -fold the total perfused medullary
3 capillary length ($P = 0.043$), ~ 2.9 -fold the number of perfused capillary segments ($P=0.02$) and ~ 2 -
4 fold the perfused volume fraction ($P=0.0031$) in medulla (Figure 2d-g). In the renal cortex,
5 hydroxyfasudil given on reperfusion increased perfusion (blood volume) ~ 1.25 -fold ($P=0.0098$;
6 Figure 1e, g), and increased the total perfused length of capillaries, the number of perfused capillary
7 segments and the blood volume fraction to values that were not significantly different from those in
8 non-ischemic kidneys (Figure 3c-f).

9 **Improvements of renal blood flow by hydroxyfasudil are via pericytes, not arterioles**

10 Hydroxyfasudil might act on arteriolar smooth muscle or pericytes, or both. However, it had
11 no effect on the diameter of afferent or efferent arterioles feeding and leaving the glomeruli (Figure
12 3h, i). In contrast, hydroxyfasudil reduced the constriction evoked at DVR pericyte somata by
13 ischemia and reperfusion, increasing the diameter from $4.5 \pm 0.5 \mu\text{m}$ without hydroxyfasudil to 8.0 ± 0.4
14 μm with the drug ($p < 0.0001$) (Figure 4g), and reduced the percentage of DVR capillaries blocked
15 from $78 \pm 9\%$ to $8 \pm 5\%$ ($P=0.023$), both of which are not significantly different from the values in non-
16 ischemic kidneys (Figure 4d, f). Thus, ischemia induces, and hydroxyfasudil decreases, medullary no-
17 reflow by specifically acting on DVR capillary pericytes rather than on upstream arterioles.

18 **Rho kinase inhibition reduces myosin light chain phosphorylation after ischemia**

19 Rho kinase can inhibit (Riddick et al., 2008; Wang et al., 2009) myosin light chain
20 phosphatase (MLCP), thus increasing phosphorylation of myosin light chain (MLC) by myosin light
21 chain kinase (MLCK) and increasing pericyte contraction, but it also has other functions. To
22 investigate how Rho kinase inhibition has the effects described above, we labelled for phosphorylated
23 MLC. After ischemia and reperfusion, this was increased ~ 11 -fold for medullary and 5-fold for
24 cortical pericytes ($P=0.0001$ in both locations, Figure 6a-j). Hydroxyfasudil treatment after
25 reperfusion reduced this increase so that the labelling was not significantly different from that in
26 control kidneys ($P=0.95$ and $P=0.56$ respectively; Figure 6a-j). Thus, if pericyte contraction is via
27 conventional smooth muscle actomyosin, the reduced MLC phosphorylation could explain pericyte

1 relaxation evoked by Rho kinase inhibition. Consistent with pericytes employing smooth muscle
2 actomyosin, 56% of DVR pericytes near blockage sites labeled for the contractile protein α -SMA
3 (Figure 6k-n; see also Park et al., 1997). Historically, demonstrating pericyte α -SMA labeling has
4 been difficult, and a more favourable fixative might increase the percentage of cells labelled (Alarcon-
5 Martinez et al., 2018).

6 **Rho kinase inhibitor reduces reperfusion-induced acute kidney injury**

7 Kidney injury molecule-1 (Kim-1) is a sensitive and early diagnostic indicator of renal injury
8 in rodent kidney injury models (Vaidya et al., 2010), and in pathology is localized at high levels on
9 the apical membrane of the proximal tubule where the tubule is most affected (Amin et al., 2004;
10 Ichimura et al., 1998). Kim-1 levels in the proximal tubules were elevated 81-fold by ischemia and
11 reperfusion ($P=0.0004$, Figure 7a, b, d), and treatment with hydroxyfasudil during reperfusion halved
12 the Kim-1 labelling ($P=0.03$, Figure 7c, d).

13

14 **Discussion**

15 This paper demonstrates, for the first time, that the long-lasting decrease of renal blood flow
16 that follows transient ischemia is generated by pericyte-mediated constriction and block of the
17 descending vasa recta and cortical peritubular capillaries, and that this post-ischemic no-reflow can be
18 reduced pharmacologically. We found *in vivo* that sites of ischemia-evoked medullary and cortical
19 capillary block were associated with pericyte locations. Furthermore, after ischemia and reperfusion,
20 the diameters of descending vasa recta and peritubular capillaries were reduced specifically near
21 pericyte somata, which extend contractile circumferential processes around the capillaries. In contrast,
22 cortical arteriole diameters were not reduced and glomeruli remained perfused. The fact that capillary
23 diameters are reduced specifically near pericyte somata establishes that this is due to a contraction of
24 the circumferential processes of pericytes, and not (for example) due to a decrease in overall perfusion
25 pressure (which would also reduce the diameter of capillaries away from pericyte somata). Together,
26 these data establish pericyte-mediated capillary constriction as a major therapeutic target for treating
27 post-ischemic renal no-reflow.

1 Pericyte-mediated constriction of renal capillaries may reflect reduced Ca^{2+} pumping in
2 ischemia, raising $[\text{Ca}^{2+}]_i$ which activates contraction, as for CNS pericytes (Hall et al., 2014).
3 Constriction may also partly reflect a release of angiotensin II (Allred et al., 2000; Boer et al., 1997;
4 da Silveira et al., 2010; Miyata et al., 1999; Sanchez-Pozos et al., 2012; Zhang et al., 2004) and
5 endothelin 1 (Afyouni et al., 2015; Jones et al., 2020; Sanchez-Pozos et al., 2012) which raise $[\text{Ca}^{2+}]_i$
6 and Rho kinase activity (Lee et al., 2014; Shimokawa & Rashid, 2007), since we found that blocking
7 endothelin 1 receptors and, to a lesser extent, angiotensin II receptors improved post-ischemic renal
8 blood flow. Consistent with this, it has been demonstrated that vasoconstricting endothelin-A
9 (Crawford et al., 2012; Wendel et al., 2006) and the angiotensin II type 1 (AT1) (Crawford et al.,
10 2012; Miyata et al., 1999; Terada et al., 1993) receptors are located on pericytes along the descending
11 vasa recta and regulate contractility at pericyte sites (Crawford et al., 2012). Additionally, endothelin
12 1 and angiotensin II evoke potent vasoconstriction of the descending vasa recta mainly through
13 endothelin-A (Silldorff et al., 1995) and angiotensin II type 1 (AT1) (Rhinehart et al., 2003) receptors.

14 Rho kinase, a key downstream effector of both endothelin 1 and angiotensin II, inhibits the
15 MLC dephosphorylation required to relax pericytes, thus promoting constriction (Hartmann et al.,
16 2021). We found that blocking Rho kinase with hydroxyfasudil reversed ischemia-evoked pericyte-
17 mediated capillary constriction, which could explain why Rho kinase block reduces acute kidney
18 injury (Kentrup et al., 2011; Prakash et al., 2008; Teraishi et al., 2004; Versteilen et al., 2011;
19 Versteilen et al., 2006), as we have confirmed using kidney injury molecule-1 (Kim-1) as a marker
20 (Figure 7c, d). (In addition to inhibiting pericyte-mediated capillary constriction, hydroxyfasudil may
21 also reduce kidney injury by reducing microvascular leukocyte accumulation, possibly by increasing
22 the activity of endothelial nitric oxide synthase: Versteilen et al., 2011; Yamasowa et al., 2005). A
23 direct effect of Rho kinase inhibition on pericyte contractility was confirmed by demonstrating that it
24 reduced MLC phosphorylation in pericytes (Figure 6a-j) and that it increased capillary diameter
25 specifically at pericyte somata (Figure 4g) in ischemic animals, implying that the effects of Rho
26 kinase inhibition were on renal pericytes rather than an extra-renal systemic action. Hydroxyfasudil is
27 the active metabolite of fasudil, a drug that has been clinically approved in Japan since 1995 for the

1 treatment of vasospasm following subarachnoid hemorrhage (Lingor et al., 2019). Fasudil treatment
2 improves stroke outcome in animal models (Vesterinen et al., 2013) and humans (Shibuya et al.,
3 2005) and our data suggest that it may also be useful for reducing post-ischemic renal no-reflow and
4 kidney damage.

5 We considered possible non-pericyte explanations for post-ischemic capillary constriction and
6 block. Post-ischemic erythrocyte congestion in vasa recta has previously been described (Crislip et al.,
7 2017; Olof et al., 1991) however red blood cells do not physically cause the capillary blockages
8 observed after ischemia as they were associated with only a small percentage of block sites (Figure
9 S2a, b). Thus, red blood cell trapping could be a consequence rather than a cause of the blockages.
10 Leukocyte trapping may also contribute to reducing blood flow, but occurs on a longer time scale than
11 we have studied (Kelly et al., 1994; Rabb et al., 1995; Ysebaert et al., 2000). Similarly, although a
12 degradation of the eGCX has been reported after ischemia (Snoeijs et al., 2010; Song et al., 2018), we
13 found a uniform distribution of the eGCX along the vessel wall, which was not modified after
14 ischemia (Figure S2e-h), thus ruling out a causal association with capillary blockages which are
15 preferentially located near pericytes. The present study demonstrates that pericyte-mediated
16 constrictions of the descending vasa recta and cortical peritubular capillaries contribute to no-reflow
17 and kidney injury at early stages of reperfusion, however we cannot exclude the possibility that other
18 factors, such as inflammation and leukocyte infiltration (Gandolfo et al., 2009; Kelly et al., 1994;
19 Rabb et al., 1995; Ysebaert et al., 2000), or eGCX dysfunction (Bongoni et al., 2019), might also
20 contribute to post-ischemic microvascular injury at later phases of acute kidney injury. Furthermore,
21 in response to the pericyte-mediated constriction evoked by ischemia, the DVR may undergo post-
22 ischemic adaptations, releasing more nitric oxide at 48 hours post-ischemia which could reduce
23 pericyte constriction at later times after ischemia than we have studied (Zhang et al., 2018).

24 The recovery of blood flow in the medulla on renal arterial reperfusion was slower than in the
25 cortex. The regulation of renal medullary blood flow is mainly mediated by vasa recta pericytes,
26 independent of total or cortical blood flow (Pallone & Silldorff, 2001). The need for accurate flow
27 regulation in the relatively hypoxic medulla may account for pericytes on the DVR being much closer

1 together (mean separation $22.9 \pm 0.9 \mu\text{m}$) than for peritubular cortical pericytes ($41.3 \pm 2.6 \mu\text{m}$) and this
2 may, in turn, contribute to a greater pericyte-mediated restriction of blood flow after ischemia in the
3 DVR than in the cortical capillaries. Perhaps surprisingly, given our data, in post-cadaveric renal
4 transplants a better outcome has been reported for kidneys with a higher number of pericytes
5 immediately post-transplant (Kwon et al., 2008). This may, however, reflect an aspect of pericyte
6 function other than capillary constriction, such as angiogenesis and maintenance of vessel integrity
7 (Shaw et al., 2018), with these functions failing in transplanted tissue in which pericytes have already
8 died due to ischemia.

9 Rodent models of renal ischemia can employ bilateral ischemia or unilateral ischemia with or
10 without contralateral nephrectomy (Fu et al., 2018). In the present study, unilateral ischemia without
11 contralateral nephrectomy (which may occur during renal-sparing surgeries) (Hollenbeck et al., 2006;
12 Medina-Rico et al., 2018) was chosen to explore the early mechanisms of ischemia and reperfusion
13 injury while using the contralateral kidney as a paired control for potential systemic hemodynamic
14 changes that could be triggered during and after the surgical procedure. The presence of an uninjured
15 contralateral kidney reduces animal mortality during the surgical procedure, and, thus, longer
16 ischemia times can be used, resulting in more severe and reproducible injury (Fu et al., 2018; Le Clef
17 et al., 2016; Polichnowski et al., 2020; Soranno et al., 2019). Unilateral ischemia-reperfusion without
18 contralateral nephrectomy is considered a strong model to study the progression from acute renal
19 injury to long-term tubulo-interstitial fibrosis (Fu et al., 2018; Le Clef et al., 2016; Polichnowski et
20 al., 2020; Soranno et al., 2019), but we acknowledge that the model used in the present study may not
21 be similar to some clinical situations where both kidneys are injured, and there are limitations of
22 translatability from all animal models of acute kidney injury to human disease (Fu et al., 2018). A
23 limitation of our study is that all experiments were performed on male rats and mice. Female rats are
24 relatively protected against post-ischemic renal failure (Lima-Posada et al., 2017; Müller et al., 2002),
25 possibly because in male rats androgens promote ischemic kidney damage by triggering endothelin-
26 induced vascular constriction (Müller et al., 2002). However, these studies showed that sex did not

1 influence ischemia repletion-induced injury after 24 hours, but only after 7 days (Lima-Posada et al.,
2 2017; Muller et al., 2002), i.e. on a much longer time scale than we have studied.

3 In the present study, we have shown that pericyte contraction contributes to reducing cortical
4 and medullary blood flow at early stages of reperfusion. This initial pattern could also contribute to
5 the pericyte injury, detachment and capillary rarefaction observed at later stages after ischemia and
6 reperfusion (Kramann et al., 2017), which lead to further damage to the kidney (Khairoun et al., 2013;
7 Kramann et al., 2017). However, there was no evidence of pericyte detachment during the time frame
8 of the present study. Treatment from the beginning of reperfusion (to mimic a clinically-possible
9 therapeutic approach) with hydroxyfasudil, a Rho kinase inhibitor, increased medullary and cortical
10 blood flow, increased the post-ischemic diameter of DVR capillaries at pericyte locations, reduced the
11 percentage of DVR capillaries that remained blocked, and reduced kidney injury after renal
12 reperfusion. Presumably the protection of renal blood flow and downstream tissue health would be
13 even greater if hydroxyfasudil could be given before ischemia was induced (e.g. in situations such as
14 cardiac surgery and kidney transplantation, where renal ischemia might be anticipated). Thus,
15 pericytes are a novel therapeutic target for reducing no-reflow after renal ischemia. Acute kidney
16 injury caused by post-ischemic no-reflow causes significant socio-economic cost. Our identification
17 of pericyte contraction as a therapeutic target for ischemia-induced acute kidney injury should
18 contribute to the development or re-purposing of drugs that can prevent renal no-reflow.

19

1 **Methods**

2 **Study approval**

3 Experiments were performed in accordance with European Commission Directive
4 2010/63/EU and the UK Animals (Scientific Procedures) Act (1986), with approval from the UCL
5 Animal Welfare and Ethical Review Body.

6 **Animal preparation for ischemia experiments**

7 Due to the high density of kidney tissue, intravital microscopy is limited to superficial regions
8 of the cortex <100 μm deep (Sandoval & Molitoris, 2017). As the renal medulla is inaccessible for in
9 vivo imaging, we used laser Doppler flowmetry to assess blood flow changes of both kidneys or
10 within the cortex and medulla of one kidney simultaneously. Additionally, we used FITC-albumin
11 gelatin perfusion for measuring microvascular network perfusion (O'Farrell et al., 2017) in the renal
12 cortex and medulla, supplemented with high resolution images of individual capillaries to assess the
13 mechanisms underlying blood flow changes.

14 Adult male Sprague-Dawley rats (P40-50), or NG2-dsRed male mice (P100-120) expressing
15 dsRed in pericytes to allow live pericyte imaging, were anesthetized with pentobarbital sodium
16 (induction 60 mg/kg i.p.; maintenance 10-15 mg/kg/h i.v.). The femoral veins were cannulated to
17 administer anesthetic and drugs. Stable kidney perfusion was confirmed using laser Doppler probes
18 (OxyFlo™ Pro 2-channel laser Doppler, Oxford, United Kingdom) to measure blood flow in the
19 contralateral kidney throughout the experiment, and anesthesia was monitored by the absence of a
20 withdrawal response to a paw pinch. Body temperature was maintained at $37.0\pm 0.5^\circ\text{C}$ with a heating
21 pad.

22 **Renal ischemia and reperfusion**

23 Both kidneys were exposed, and the renal arteries and veins were dissected. Left kidneys
24 were subjected to 60 min ischemia by renal artery and vein cross-clamp, followed by 30 or 60 min
25 reperfusion. This reperfusion duration was chosen to assess pericyte function soon after starting
26 reperfusion. Right kidneys underwent the same procedures without vessel clamping. Two laser
27 Doppler single-fibre implantable probes of 0.5mm diameter (MSF100NX, Oxford Optronix, Oxford,

1 United Kingdom) measured simultaneously the perfusion of both kidneys (or of the outer medulla and
2 cortex of one kidney). Cortical and outer medullary perfusion were measured with the probe on or 2
3 mm below the kidney surface, respectively. Successful artery and vein occlusion was confirmed by a
4 sudden fall of laser Doppler signal. Laser Doppler monitoring, which detects the movement of cells in
5 the blood, is a widely used method for studies of microvascular perfusion in experimental and clinical
6 studies and measures the total local microcirculatory blood perfusion in capillaries, arterioles, venules
7 and shunting vessels (Fredriksson et al., 2009; Rajan et al., 2009). Laser Doppler is suitable for
8 monitoring of relative renal microvascular blood flow changes in response to physiological and
9 pharmacological stimuli in rodents (Lu et al., 1993; Vassileva et al., 2003).

10 Endothelial glycocalyx (eGCX) was labelled in vivo using wheat germ agglutinin (WGA)
11 Alexa Fluor 647 conjugate (ThermoFisher, W32466, Waltham, MA) injected through the jugular vein
12 (200 μ l, 1 mg/ml) 45 minutes before renal ischemia/reperfusion (Kutuzov et al., 2018). WGA binds to
13 N-acetyl-D-glucosamine and sialic acid residues of the eGCX. Using ImageJ, WGA fluorescence
14 intensities were measured by drawing regions of interest (ROIs) across capillaries at the mid-points of
15 pericyte somata, and away from the soma in 5 μ m increments on both sides of the pericyte. Capillary
16 diameters were also measured at each position.

17 Hydroxyfasudil hydrochloride, a reversible cell-permeable inhibitor of Rho kinase (Santa
18 Cruz Biotechnology sc-202176, Dallas, TX) which is expected to decrease pericyte contractility
19 (Hartmann et al., 2021; Kutcher et al., 2007) was administered as a bolus (3 mg/kg *i.v.*), immediately
20 on starting reperfusion. This protocol, rather than having the drug present during the ischemic insult,
21 better mimics a clinical situation where drugs could be given on reperfusion. Control and non-treated
22 ischemic animals received saline infusion with the same volume.

23 **Animal perfusion and tissue preparation for imaging**

24 After renal ischemia/reperfusion, animals were overdosed with pentobarbital sodium and
25 transcardially-perfused with phosphate-buffered saline (PBS) (200 ml) followed by 4%
26 paraformaldehyde (PFA, 200 ml) fixative and then 5% gelatin (20ml in PBS Sigma-Aldrich, G2625,
27 Darmstadt, Germany) solution containing FITC-albumin (Sigma-Aldrich, A9771, Darmstadt,

1 Germany), followed by immersion in ice for 30 minutes (adapted from (Blinder et al., 2013)).
2 Kidneys were fixed overnight in 4% PFA, and 150 μm longitudinal sections made for
3 immunohistochemistry. Rats have ~64 ml of blood per kg bodyweight, thus the FITC-albumin gelatin
4 solution would suffice to fill the total blood volume. The gelatin sets when the body temperature falls
5 and traps FITC-albumin in the perfused vessels; blocked vessels show no penetration of FITC-
6 albumin past the block.

7 **In vivo two-photon imaging**

8 NG2-DsRed mice (P100-120) were anesthetized using urethane (1.55 g/kg i.p., in two doses
9 15 min apart). Anesthesia was confirmed by the absence of a paw pinch withdrawal response. Body
10 temperature was maintained at $36.8\pm 0.3^\circ\text{C}$. A custom-built plate, attached to the kidney using
11 superglue and agarose created a sealed well filled with phosphate-buffered saline during imaging,
12 when the plate was secured under the objective on a custom-built stage.

13 Peritubular capillary diameter was recorded during renal ischemia/reperfusion using two-
14 photon microscopy of the intraluminal FITC-albumin (1 mg in 100 μl of saline given intravenously).
15 Two-photon excitation used a Newport-Spectra Physics Mai Tai Ti:Sapphire Laser pulsing at 80
16 MHz, and a (Zeiss LSM710, Oberkochen, Germany) microscope with a 20 \times water immersion
17 objective (NA 1.0). Fluorescence was excited using 920 nm wavelength for DsRed, and 820 nm for
18 FITC-albumin and Hoechst 33342. Mean laser power under the objective was <35 mW. Images were
19 analysed using ImageJ. Vessel diameter was defined using a line drawn across the vessel as the width
20 of the intraluminal dye fluorescence.

21 **Immunohistochemistry**

22 Pericytes were labelled by expression of DsRed under control of the NG2 promoter (in mice), or with
23 antibodies to NG2 (1:200; Abcam ab50009, Cambridge, United Kingdom), α -smooth muscle actin (α -
24 SMA) (1:100; Abcam ab5694, Cambridge, United Kingdom), or myosin light chain (phospho S20,
25 1:100, Abcam ab2480, Cambridge, United Kingdom), and the capillary basement membrane and
26 pericytes were labelled with isolectin B₄-Alexa Fluor 647 (1:200, overnight; Molecular Probes,
27 I32450, Thermo Fisher Scientific, Waltham, MA). Z-stacks of the cortex and outer medulla (frame
28 size 640.17x640.17 μm) for cell counting were acquired confocally (Zeiss LSM 700, Oberkochen,

1 Germany). Pericyte intersoma distance was calculated between pairs of pericytes on capillaries within
2 the same imaging plane. Kidney damage was assessed using kidney injury molecule-1 (Kim-1)
3 antibody (1:100, overnight; Novus Biologicals, NBP1-76701, Abingdon, United Kingdom). Red
4 blood cells were labelled with antibody to glycophorin A (1:2000, AbCam ab9520, Cambridge,
5 United Kingdom). Alexa Fluor conjugated secondary antibodies were added overnight (1:500;
6 ThermoFisher, A31572, A31556, A31570, Waltham, MA).

7 **Image analysis**

8 Regions of interest (ROIs) were drawn around the renal cortex and medulla (Fig. 1), and the
9 mean FITC-albumin signal intensity was measured for each ROI using ImageJ. This signal is assumed
10 to provide an approximate measure of the amount of blood perfusing the tissue (conceivably
11 downstream capillary constriction could lead to an upstream dilation and an increased blood volume
12 being detected but, if this did occur, it would lead to an underestimate of the decrease of perfusion
13 occurring). To gain a more accurate assessment of perfusion, we also used the ImageJ macro
14 TubeAnalyst to measure the microvascular network of the renal cortex and medulla and obtain the
15 total perfused capillary length, the number of perfused capillary segments and the overall perfused
16 microvascular volume fraction. To quantify the percentage of perfused capillaries, we counted the
17 number of filled (with FITC-albumin) and unfilled vessels that crossed a line drawn through the
18 centre of each image perpendicular to the main capillary axis.

19 To assess whether pericytes cause flow blockages, we measured the distance along the
20 capillary from the termination of the FITC-albumin signal to the mid-point of the nearest visible
21 pericyte soma, since in brain most contractile circumferential pericyte processes (which can adjust
22 capillary diameter) are near the pericyte soma (see Figures 4d, 5f, S2 and S3 of Ref (Nortley et al.,
23 2019)). Capillary diameters were measured at the block sites where the FITC-albumin signal
24 terminated. We also plotted the diameter of the FITC-albumin labelled capillary lumen as a function
25 of the distance from the pericyte somata to assess whether diameter reduction was a nonspecific effect
26 of ischemia, or was pericyte-related. A constriction seen specifically at pericyte somata is an
27 unambiguous indication that pericyte contraction is occurring (Nortley et al., 2019). The

1 identification, and direction of flow, of the afferent and efferent arterioles were deduced from tracking
2 in confocal Z-stacks.

3 **Statistics**

4 Statistical analysis employed Graphpad Prism (San Diego, CA). Data normality was tested
5 with Shapiro-Wilk tests. Normally distributed data were compared using Student's 2-tailed t-tests or
6 ANOVA tests. Data that were not normally distributed were analysed with Mann-Whitney or
7 Kruskal-Wallis tests. *P* values were corrected for multiple comparisons using a procedure equivalent
8 to the Holm-Bonferroni method or Dunn's test (corrected *P* values are significant if they are less than
9 0.05).

10

1 **Author contributions**

2 FF devised experiments, carried them out, analysed data and wrote the first draft of the paper.

3 DA helped to devise experiments and analyse data, and edited the paper.

4

5 **Acknowledgments**

6 We thank Jonathan Lezmy, Svetlana Mastitskaya and Thomas Pfeiffer for comments on the
7 manuscript.

8

9 **Competing interests**

10 The authors declare no conflicts of interest.

11

12 **Funding**

13 Supported by a Rosetrees Trust and Stoneygate Trust grant to DA and FF, and equipment
14 funded by the Wellcome Trust and European Research Council.

15

16

17

1 **References**

- 2 Afyouni, N. E., Halili, H., Moslemi, F., Nematbakhsh, M., Talebi, A., Shirdavani, S., & Maleki, M.
3 (2015). Preventive Role of Endothelin Antagonist on Kidney Ischemia: Reperfusion Injury in
4 Male and Female Rats. *Int J Prev Med*, 6, 128. <https://doi.org/10.4103/2008-7802.172549>
- 5 Alarcon-Martinez, L., Yilmaz-Ozcan, S., Yemisci, M., Schallek, J., Kilic, K., Can, A., . . . Dalkara, T.
6 (2018). Capillary pericytes express alpha-smooth muscle actin, which requires prevention of
7 filamentous-actin depolymerization for detection. *Elife*, 7.
8 <https://doi.org/10.7554/eLife.34861>
- 9 Allred, A. J., Chappell, M. C., Ferrario, C. M., & Diz, D. I. (2000). Differential actions of renal
10 ischemic injury on the intrarenal angiotensin system. *Am J Physiol Renal Physiol*, 279(4),
11 F636-645. <https://doi.org/10.1152/ajprenal.2000.279.4.F636>
- 12 Amin, R. P., Vickers, A. E., Sistare, F., Thompson, K. L., Roman, R. J., Lawton, M., . . . Afshari, C.
13 A. (2004). Identification of putative gene based markers of renal toxicity. *Environ Health*
14 *Perspect*, 112(4), 465-479. <https://doi.org/10.1289/ehp.6683>
- 15 Blinder, P., Tsai, P. S., Kaufhold, J. P., Knutsen, P. M., Suhl, H., & Kleinfeld, D. (2013). The cortical
16 angiome: an interconnected vascular network with noncolumnar patterns of blood flow. *Nat*
17 *Neurosci*, 16(7), 889-897. <https://doi.org/10.1038/nn.3426>
- 18 Boer, W. H., Braam, B., Fransen, R., Boer, P., & Koomans, H. A. (1997). Effects of reduced renal
19 perfusion pressure and acute volume expansion on proximal tubule and whole kidney
20 angiotensin II content in the rat. *Kidney Int*, 51(1), 44-49. <https://doi.org/10.1038/ki.1997.6>
- 21 Bongoni, A. K., Lu, B., McRae, J. L., Salvaris, E. J., Toonen, E. J. M., Vikstrom, I., . . . Cowan, P. J.
22 (2019). Complement-mediated Damage to the Glycocalyx Plays a Role in Renal Ischemia-
23 reperfusion Injury in Mice. *Transplant Direct*, 5(4), e341.
24 <https://doi.org/10.1097/TXD.0000000000000881>
- 25 Bonventre, J. V., & Weinberg, J. M. (2003). Recent advances in the pathophysiology of ischemic
26 acute renal failure. *J Am Soc Nephrol*, 14(8), 2199-2210.
27 <https://doi.org/10.1097/01.asn.0000079785.13922.f6>

- 1 Conesa, E. L., Valero, F., Nadal, J. C., Fenoy, F. J., Lopez, B., Arregui, B., & Salom, M. G. (2001).
2 N-acetyl-L-cysteine improves renal medullary hypoperfusion in acute renal failure. *Am J*
3 *Physiol Regul Integr Comp Physiol*, 281(3), R730-737.
4 <https://doi.org/10.1152/ajpregu.2001.281.3.R730>
- 5 Crawford, C., Kennedy-Lydon, T., Sprott, C., Desai, T., Sawbridge, L., Munday, J., . . . Peppiatt-
6 Wildman, C. M. (2012). An intact kidney slice model to investigate vasa recta properties and
7 function in situ. *Nephron Physiol*, 120(3), p17-31. <https://doi.org/10.1159/000339110>
- 8 Crislip, G. R., O'Connor, P. M., Wei, Q., & Sullivan, J. C. (2017). Vasa recta pericyte density is
9 negatively associated with vascular congestion in the renal medulla following ischemia
10 reperfusion in rats. *Am J Physiol Renal Physiol*, 313(5), F1097-f1105.
11 <https://doi.org/10.1152/ajprenal.00261.2017>
- 12 Cristol, J. P., Thiernemann, C., Guerin, M. C., Torreilles, J., & de Paulet, A. C. (1996). L-Arginine
13 infusion after ischaemia-reperfusion of rat kidney enhances lipid peroxidation. *J Lipid Mediat*
14 *Cell Signal*, 13(1), 9-17. [https://doi.org/10.1016/0929-7855\(95\)00010-0](https://doi.org/10.1016/0929-7855(95)00010-0)
- 15 da Silveira, K. D., Pompermayer Bosco, K. S., Diniz, L. R., Carmona, A. K., Cassali, G. D., Bruna-
16 Romero, O., . . . Ribeiro Vieira, M. A. (2010). ACE2-angiotensin-(1-7)-Mas axis in renal
17 ischaemia/reperfusion injury in rats. *Clin Sci (Lond)*, 119(9), 385-394.
18 <https://doi.org/10.1042/cs20090554>
- 19 Durham, J. T., Surks, H. K., Dulmovits, B. M., & Herman, I. M. (2014). Pericyte contractility controls
20 endothelial cell cycle progression and sprouting: insights into angiogenic switch mechanics.
21 *Am J Physiol Cell Physiol*, 307(9), C878-892. <https://doi.org/10.1152/ajpcell.00185.2014>
- 22 Fredriksson, I., Larsson, M., & Stromberg, T. (2009). Measurement depth and volume in laser
23 Doppler flowmetry. *Microvasc Res*, 78(1), 4-13. <https://doi.org/10.1016/j.mvr.2009.02.008>
- 24 Fu, Y., Tang, C., Cai, J., Chen, G., Zhang, D., & Dong, Z. (2018). Rodent models of AKI-CKD
25 transition. *Am J Physiol Renal Physiol*, 315(4), F1098-f1106.
26 <https://doi.org/10.1152/ajprenal.00199.2018>

- 1 Gameiro, J., Agapito Fonseca, J., Jorge, S., & Lopes, J. A. (2018). Acute Kidney Injury Definition
2 and Diagnosis: A Narrative Review. *J Clin Med*, 7(10). <https://doi.org/10.3390/jcm7100307>
- 3 Gandolfo, M. T., Jang, H. R., Bagnasco, S. M., Ko, G. J., Agreda, P., Satpute, S. R., . . . Rabb, H.
4 (2009). Foxp3+ regulatory T cells participate in repair of ischemic acute kidney injury.
5 *Kidney Int*, 76(7), 717-729. <https://doi.org/10.1038/ki.2009.259>
- 6 Hall, C. N., Reynell, C., Gesslein, B., Hamilton, N. B., Mishra, A., Sutherland, B. A., . . . Attwell, D.
7 (2014). Capillary pericytes regulate cerebral blood flow in health and disease. *Nature*,
8 508(7494), 55-60. <https://doi.org/10.1038/nature13165>
- 9 Hartmann, D. A., Berthiaume, A. A., Grant, R. I., Harrill, S. A., Koski, T., Tieu, T., . . . Shih, A. Y.
10 (2021). Brain capillary pericytes exert a substantial but slow influence on blood flow. *Nat*
11 *Neurosci*, 24(5), 633-645. <https://doi.org/10.1038/s41593-020-00793-2>
- 12 Hirunpattarasilp, C., Attwell, D., & Freitas, F. (2019). The role of pericytes in brain disorders: from
13 the periphery to the brain. *J Neurochem*, 150(6), 648-665. <https://doi.org/10.1111/jnc.14725>
- 14 Hollenbeck, B. K., Taub, D. A., Miller, D. C., Dunn, R. L., & Wei, J. T. (2006). National utilization
15 trends of partial nephrectomy for renal cell carcinoma: a case of underutilization? *Urology*,
16 67(2), 254-259. <https://doi.org/10.1016/j.urology.2005.08.050>
- 17 Homma, K., Hayashi, K., Wakino, S., Tokuyama, H., Kanda, T., Tatematsu, S., . . . Itoh, H. (2014).
18 Rho-kinase contributes to pressure-induced constriction of renal microvessels. *Keio J Med*,
19 63(1), 1-12. <https://www.ncbi.nlm.nih.gov/pubmed/24429483>
- 20 Hoste, E. A. J., Kellum, J. A., Selby, N. M., Zarbock, A., Palevsky, P. M., Bagshaw, S. M., . . .
21 Chawla, L. S. (2018). Global epidemiology and outcomes of acute kidney injury. *Nat Rev*
22 *Nephrol*, 14(10), 607-625. <https://doi.org/10.1038/s41581-018-0052-0>
- 23 Ichimura, T., Bonventre, J. V., Bailly, V., Wei, H., Hession, C. A., Cate, R. L., & Sanicola, M.
24 (1998). Kidney injury molecule-1 (KIM-1), a putative epithelial cell adhesion molecule
25 containing a novel immunoglobulin domain, is up-regulated in renal cells after injury. *J Biol*
26 *Chem*, 273(7), 4135-4142. <https://doi.org/10.1074/jbc.273.7.4135>

- 1 Jones, N. K., Stewart, K., Czopek, A., Menzies, R. I., Thomson, A., Moran, C. M., . . . Bailey, M. A.
2 (2020). Endothelin-1 Mediates the Systemic and Renal Hemodynamic Effects of GPR81
3 Activation. *Hypertension*, *75*(5), 1213-1222.
4 <https://doi.org/10.1161/HYPERTENSIONAHA.119.14308>
- 5 Kelly, K. J., Williams, W. W., Jr., Colvin, R. B., & Bonventre, J. V. (1994). Antibody to intercellular
6 adhesion molecule 1 protects the kidney against ischemic injury. *Proc Natl Acad Sci U S A*,
7 *91*(2), 812-816. <https://doi.org/10.1073/pnas.91.2.812>
- 8 Kentrup, D., Reuter, S., Schnockel, U., Grabner, A., Edemir, B., Pavenstadt, H., . . . Bussemaker, E.
9 (2011). Hydroxyfasudil-mediated inhibition of ROCK1 and ROCK2 improves kidney
10 function in rat renal acute ischemia-reperfusion injury. *PLoS One*, *6*(10), e26419.
11 <https://doi.org/10.1371/journal.pone.0026419>
- 12 Khairoun, M., van der Pol, P., de Vries, D. K., Lievers, E., Schlagwein, N., de Boer, H. C., . . .
13 Reinders, M. E. (2013). Renal ischemia-reperfusion induces a dysbalance of angiopoietins,
14 accompanied by proliferation of pericytes and fibrosis. *Am J Physiol Renal Physiol*, *305*(6),
15 F901-910. <https://doi.org/10.1152/ajprenal.00542.2012>
- 16 Kramann, R., Wongboonsin, J., Chang-Panesso, M., Machado, F. G., & Humphreys, B. D. (2017).
17 Gli1(+) Pericyte Loss Induces Capillary Rarefaction and Proximal Tubular Injury. *J Am Soc*
18 *Nephrol*, *28*(3), 776-784. <https://doi.org/10.1681/asn.2016030297>
- 19 Kutcher, M. E., Kolyada, A. Y., Surks, H. K., & Herman, I. M. (2007). Pericyte Rho GTPase
20 mediates both pericyte contractile phenotype and capillary endothelial growth state. *Am J*
21 *Pathol*, *171*(2), 693-701. <https://doi.org/10.2353/ajpath.2007.070102>
- 22 Kutuzov, N., Flyvbjerg, H., & Lauritzen, M. (2018). Contributions of the glycocalyx, endothelium,
23 and extravascular compartment to the blood-brain barrier. *Proc Natl Acad Sci U S A*, *115*(40),
24 E9429-e9438. <https://doi.org/10.1073/pnas.1802155115>
- 25 Kwon, O., Hong, S. M., Sutton, T. A., & Temm, C. J. (2008). Preservation of peritubular capillary
26 endothelial integrity and increasing pericytes may be critical to recovery from postischemic

- 1 acute kidney injury. *Am J Physiol Renal Physiol*, 295(2), F351-359.
2 <https://doi.org/10.1152/ajprenal.90276.2008>
- 3 Lameire, N., Van Biesen, W., & Vanholder, R. (2006). The changing epidemiology of acute renal
4 failure. *Nat Clin Pract Nephrol*, 2(7), 364-377. <https://doi.org/10.1038/ncpneph0218>
- 5 Lameire, N., & Vanholder, R. (2001). Pathophysiologic features and prevention of human and
6 experimental acute tubular necrosis. *J Am Soc Nephrol*, 12 Suppl 17, S20-32.
7 <https://www.ncbi.nlm.nih.gov/pubmed/11251028>
- 8 Le Clef, N., Verhulst, A., D'Haese, P. C., & Vervaeet, B. A. (2016). Unilateral Renal Ischemia-
9 Reperfusion as a Robust Model for Acute to Chronic Kidney Injury in Mice. *PLoS One*,
10 11(3), e0152153. <https://doi.org/10.1371/journal.pone.0152153>
- 11 Lee, T. M., Chung, T. H., Lin, S. Z., & Chang, N. C. (2014). Endothelin receptor blockade
12 ameliorates renal injury by inhibition of RhoA/Rho-kinase signalling in deoxycorticosterone
13 acetate-salt hypertensive rats. *J Hypertens*, 32(4), 795-805.
14 <https://doi.org/10.1097/HJH.0000000000000092>
- 15 Lima-Posada, I., Portas-Cortes, C., Perez-Villalva, R., Fontana, F., Rodriguez-Romo, R., Prieto, R., . .
16 . Bobadilla, N. A. (2017). Gender Differences in the Acute Kidney Injury to Chronic Kidney
17 Disease Transition. *Sci Rep*, 7(1), 12270. <https://doi.org/10.1038/s41598-017-09630-2>
- 18 Lingor, P., Weber, M., Camu, W., Friede, T., Hilgers, R., Leha, A., . . . Investigators, R.-A. (2019).
19 ROCK-ALS: Protocol for a Randomized, Placebo-Controlled, Double-Blind Phase IIa Trial
20 of Safety, Tolerability and Efficacy of the Rho Kinase (ROCK) Inhibitor Fasudil in
21 Amyotrophic Lateral Sclerosis. *Front Neurol*, 10, 293.
22 <https://doi.org/10.3389/fneur.2019.00293>
- 23 Lu, S., Mattson, D. L., Roman, R. J., Becker, C. G., & Cowley, A. W., Jr. (1993). Assessment of
24 changes in intrarenal blood flow in conscious rats using laser-Doppler flowmetry. *Am J*
25 *Physiol*, 264(6 Pt 2), F956-962. <https://doi.org/10.1152/ajprenal.1993.264.6.F956>
- 26 McCurley, A., Alimperti, S., Campos-Bilderback, S. B., Sandoval, R. M., Calvino, J. E., Reynolds, T.
27 L., . . . Crackower, M. A. (2017). Inhibition of alphavbeta5 Integrin Attenuates Vascular

- 1 Permeability and Protects against Renal Ischemia-Reperfusion Injury. *J Am Soc Nephrol*,
2 28(6), 1741-1752. <https://doi.org/10.1681/ASN.2016020200>
- 3 Medina-Rico, M., Ramos, H. L., Lobo, M., Romo, J., & Prada, J. G. (2018). Epidemiology of renal
4 cancer in developing countries: Review of the literature. *Can Urol Assoc J*, 12(3), E154-e162.
5 <https://doi.org/10.5489/cuaj.4464>
- 6 Mehta, R. L., Burdmann, E. A., Cerda, J., Feehally, J., Finkelstein, F., Garcia-Garcia, G., . . .
7 Remuzzi, G. (2016). Recognition and management of acute kidney injury in the International
8 Society of Nephrology 0by25 Global Snapshot: a multinational cross-sectional study. *Lancet*,
9 387(10032), 2017-2025. [https://doi.org/10.1016/S0140-6736\(16\)30240-9](https://doi.org/10.1016/S0140-6736(16)30240-9)
- 10 Miyata, N., Park, F., Li, X. F., & Cowley, A. W., Jr. (1999). Distribution of angiotensin AT1 and AT2
11 receptor subtypes in the rat kidney. *Am J Physiol*, 277(3), F437-446.
12 <https://doi.org/10.1152/ajprenal.1999.277.3.F437>
- 13 Muller, V., Losonczy, G., Heemann, U., Vannay, A., Fekete, A., Reusz, G., . . . Szabo, A. J. (2002).
14 Sexual dimorphism in renal ischemia-reperfusion injury in rats: possible role of endothelin.
15 *Kidney Int*, 62(4), 1364-1371. <https://doi.org/10.1111/j.1523-1755.2002.kid590.x>
- 16 Nijveldt, R. J., Prins, H. A., van Kemenade, F. J., Teerlink, T., van Lambalgen, A. A., Boelens, P. G.,
17 . . . van Leeuwen, P. A. (2001). Low arginine plasma levels do not aggravate renal blood flow
18 after experimental renal ischaemia/reperfusion. *Eur J Vasc Endovasc Surg*, 22(3), 232-239.
19 <https://doi.org/10.1053/ejvs.2001.1444>
- 20 Nortley, R., Korte, N., Izquierdo, P., Hirunpattarasilp, C., Mishra, A., Jaunmuktane, Z., . . . Attwell,
21 D. (2019). Amyloid beta oligomers constrict human capillaries in Alzheimer's disease via
22 signaling to pericytes. *Science*, 365(6450). <https://doi.org/10.1126/science.aav9518>
- 23 O'Farrell, F. M., Mastitskaya, S., Hammond-Haley, M., Freitas, F., Wah, W. R., & Attwell, D. (2017).
24 Capillary pericytes mediate coronary no-reflow after myocardial ischaemia. *Elife*, 6.
25 <https://doi.org/10.7554/eLife.29280>

- 1 Olof, P., Hellberg, A., Kallskog, O., & Wolgast, M. (1991). Red cell trapping and postischemic renal
2 blood flow. Differences between the cortex, outer and inner medulla. *Kidney Int*, 40(4), 625-
3 631. <https://doi.org/10.1038/ki.1991.254>
- 4 Pallone, T. L., & Silldorff, E. P. (2001). Pericyte regulation of renal medullary blood flow. *Exp*
5 *Nephrol*, 9(3), 165-170. <https://doi.org/10.1159/000052608>
- 6 Park, F., Mattson, D. L., Roberts, L. A., & Cowley, A. W., Jr. (1997). Evidence for the presence of
7 smooth muscle alpha-actin within pericytes of the renal medulla. *Am J Physiol*, 273(5),
8 R1742-1748. <https://doi.org/10.1152/ajpregu.1997.273.5.R1742>
- 9 Polichnowski, A. J., Griffin, K. A., Licea-Vargas, H., Lan, R., Picken, M. M., Long, J., . . . Bidani, A.
10 K. (2020). Pathophysiology of unilateral ischemia-reperfusion injury: importance of renal
11 counterbalance and implications for the AKI-CKD transition. *Am J Physiol Renal Physiol*,
12 318(5), F1086-f1099. <https://doi.org/10.1152/ajprenal.00590.2019>
- 13 Ponce, D., & Balbi, A. (2016). Acute kidney injury: risk factors and management challenges in
14 developing countries. *Int J Nephrol Renovasc Dis*, 9, 193-200.
15 <https://doi.org/10.2147/ijnrd.s104209>
- 16 Prakash, J., de Borst, M. H., Lacombe, M., Opdam, F., Klok, P. A., van Goor, H., . . . Kok, R. J.
17 (2008). Inhibition of renal rho kinase attenuates ischemia/reperfusion-induced injury. *J Am*
18 *Soc Nephrol*, 19(11), 2086-2097. <https://doi.org/10.1681/ASN.2007070794>
- 19 Rabb, H., Mendiola, C. C., Saba, S. R., Dietz, J. R., Smith, C. W., Bonventre, J. V., & Ramirez, G.
20 (1995). Antibodies to ICAM-1 protect kidneys in severe ischemic reperfusion injury. *Biochem*
21 *Biophys Res Commun*, 211(1), 67-73. <https://doi.org/10.1006/bbrc.1995.1779>
- 22 Rajan, V., Varghese, B., van Leeuwen, T. G., & Steenbergen, W. (2009). Review of methodological
23 developments in laser Doppler flowmetry. *Lasers Med Sci*, 24(2), 269-283.
24 <https://doi.org/10.1007/s10103-007-0524-0>
- 25 Ramaswamy, D., Corrigan, G., Polhemus, C., Boothroyd, D., Scandling, J., Sommer, F. G., . . .
26 Myers, B. D. (2002). Maintenance and recovery stages of postischemic acute renal failure in

- 1 humans. *Am J Physiol Renal Physiol*, 282(2), F271-280.
2 <https://doi.org/10.1152/ajprenal.0068.2001>
- 3 Regner, K. R., Zuk, A., Van Why, S. K., Shames, B. D., Ryan, R. P., Falck, J. R., . . . Roman, R. J.
4 (2009). Protective effect of 20-HETE analogues in experimental renal ischemia reperfusion
5 injury. *Kidney Int*, 75(5), 511-517. <https://doi.org/10.1038/ki.2008.600>
- 6 Rhinehart, K., Handelsman, C. A., Silldorff, E. P., & Pallone, T. L. (2003). ANG II AT2 receptor
7 modulates AT1 receptor-mediated descending vasa recta endothelial Ca²⁺ signaling. *Am J*
8 *Physiol Heart Circ Physiol*, 284(3), H779-789. <https://doi.org/10.1152/ajpheart.00317.2002>
- 9 Riddick, N., Ohtani, K., & Surks, H. K. (2008). Targeting by myosin phosphatase-RhoA interacting
10 protein mediates RhoA/ROCK regulation of myosin phosphatase. *J Cell Biochem*, 103(4),
11 1158-1170. <https://doi.org/10.1002/jcb.21488>
- 12 Ronco, C., Reis, T., & Husain-Syed, F. (2020). Management of acute kidney injury in patients with
13 COVID-19. *Lancet Respir Med*. [https://doi.org/10.1016/S2213-2600\(20\)30229-0](https://doi.org/10.1016/S2213-2600(20)30229-0)
- 14 Sanchez-Pozos, K., Barrera-Chimal, J., Garzon-Muvdi, J., Perez-Villalva, R., Rodriguez-Romo, R.,
15 Cruz, C., . . . Bobadilla, N. A. (2012). Recovery from ischemic acute kidney injury by
16 spironolactone administration. *Nephrol Dial Transplant*, 27(8), 3160-3169.
17 <https://doi.org/10.1093/ndt/gfs014>
- 18 Sandoval, R. M., & Molitoris, B. A. (2017). Intravital multiphoton microscopy as a tool for studying
19 renal physiology and pathophysiology. *Methods*, 128, 20-32.
20 <https://doi.org/10.1016/j.ymeth.2017.07.014>
- 21 Shaw, I., Rider, S., Mullins, J., Hughes, J., & Péault, B. (2018) Pericytes in the renal vasculature:
22 roles in health and disease. *Nat Rev Nephrol*, 14, 521-534. DOI: 10.1038/s41581-018-0032-4
- 23 Shibuya, M., Hirai, S., Seto, M., Satoh, S., & Ohtomo, E. (2005). Effects of fasudil in acute ischemic
24 stroke: results of a prospective placebo-controlled double-blind trial. *J Neurol Sci*, 238(1-2),
25 31-39. <https://doi.org/10.1016/j.jns.2005.06.003>
- 26 Shimokawa, H., & Rashid, M. (2007). Development of Rho-kinase inhibitors for cardiovascular
27 medicine. *Trends Pharmacol Sci*, 28(6), 296-302. <https://doi.org/10.1016/j.tips.2007.04.006>

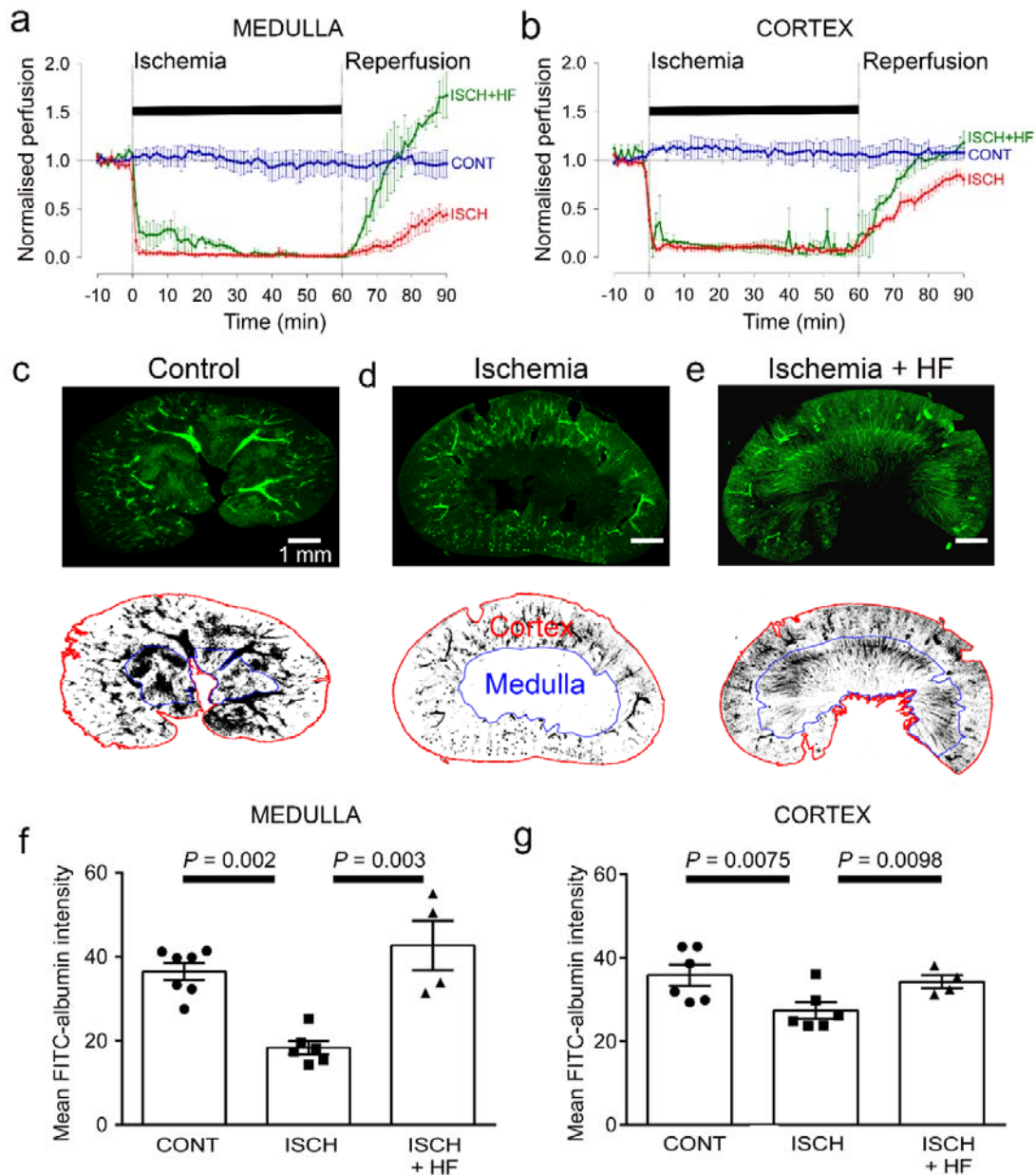
- 1 Silldorff, E. P., Yang, S., & Pallone, T. L. (1995). Prostaglandin E2 abrogates endothelin-induced
2 vasoconstriction in renal outer medullary descending vasa recta of the rat. *J Clin Invest*, *95*(6),
3 2734-2740. <https://doi.org/10.1172/jci117976>
- 4 Snoeijs, M. G., Vink, H., Voesten, N., Christiaans, M. H., Daemen, J. W., Peppelenbosch, A. G., . . .
5 van Heurn, L. W. (2010). Acute ischemic injury to the renal microvasculature in human
6 kidney transplantation. *Am J Physiol Renal Physiol*, *299*(5), F1134-1140.
7 <https://doi.org/10.1152/ajprenal.00158.2010>
- 8 Song, J. W., Zullo, J., Lipphardt, M., Dragovich, M., Zhang, F. X., Fu, B., & Goligorsky, M. S.
9 (2018). Endothelial glycocalyx-the battleground for complications of sepsis and kidney
10 injury. *Nephrol Dial Transplant*, *33*(2), 203-211. <https://doi.org/10.1093/ndt/gfx076>
- 11 Soranno, D. E., Gil, H. W., Kirkbride-Romeo, L., Altmann, C., Montford, J. R., Yang, H., . . . Faubel,
12 S. (2019). Matching Human Unilateral AKI, a Reverse Translational Approach to Investigate
13 Kidney Recovery after Ischemia. *J Am Soc Nephrol*, *30*(6), 990-1005.
14 <https://doi.org/10.1681/ASN.2018080808>
- 15 Sutton, T. A., Fisher, C. J., & Molitoris, B. A. (2002). Microvascular endothelial injury and
16 dysfunction during ischemic acute renal failure. *Kidney Int*, *62*(5), 1539-1549.
17 <https://doi.org/10.1046/j.1523-1755.2002.00631.x>
- 18 Terada, Y., Tomita, K., Nonoguchi, H., & Marumo, F. (1993). PCR localization of angiotensin II
19 receptor and angiotensinogen mRNAs in rat kidney. *Kidney Int*, *43*(6), 1251-1259.
20 <https://doi.org/10.1038/ki.1993.177>
- 21 Teraishi, K., Kurata, H., Nakajima, A., Takaoka, M., & Matsumura, Y. (2004). Preventive effect of
22 Y-27632, a selective Rho-kinase inhibitor, on ischemia/reperfusion-induced acute renal
23 failure in rats. *Eur J Pharmacol*, *505*(1-3), 205-211.
24 <https://doi.org/10.1016/j.ejphar.2004.10.040>
- 25 Vaidya, V. S., Ozer, J. S., Dieterle, F., Collings, F. B., Ramirez, V., Troth, S., . . . Bonventre, J. V.
26 (2010). Kidney injury molecule-1 outperforms traditional biomarkers of kidney injury in

- 1 preclinical biomarker qualification studies. *Nat Biotechnol*, 28(5), 478-485.
2 <https://doi.org/10.1038/nbt.1623>
- 3 Vassileva, I., Mountain, C., & Pollock, D. M. (2003). Functional role of ETB receptors in the renal
4 medulla. *Hypertension*, 41(6), 1359-1363.
5 <https://doi.org/10.1161/01.hyp.0000070958.39174.7e>
- 6 Versteilen, A. M., Blaauw, N., Di Maggio, F., Groeneveld, A. B., Sipkema, P., Musters, R. J., &
7 Tangelder, G. J. (2011). rho-Kinase inhibition reduces early microvascular leukocyte
8 accumulation in the rat kidney following ischemia-reperfusion injury: roles of nitric oxide and
9 blood flow. *Nephron Exp Nephrol*, 118(4), e79-86. <https://doi.org/10.1159/000322605>
- 10 Versteilen, A. M., Korstjens, I. J., Musters, R. J., Groeneveld, A. B., & Sipkema, P. (2006). Rho
11 kinase regulates renal blood flow by modulating eNOS activity in ischemia-reperfusion of the
12 rat kidney. *Am J Physiol Renal Physiol*, 291(3), F606-611.
13 <https://doi.org/10.1152/ajprenal.00434.2005>
- 14 Vesterinen, H. M., Currie, G. L., Carter, S., Mee, S., Watzlawick, R., Egan, K. J., . . . Sena, E. S.
15 (2013). Systematic review and stratified meta-analysis of the efficacy of RhoA and Rho
16 kinase inhibitors in animal models of ischaemic stroke. *Syst Rev*, 2, 33.
17 <https://doi.org/10.1186/2046-4053-2-33>
- 18 Wang, Y., Zheng, X. R., Riddick, N., Bryden, M., Baur, W., Zhang, X., & Surks, H. K. (2009).
19 ROCK isoform regulation of myosin phosphatase and contractility in vascular smooth muscle
20 cells. *Circ Res*, 104(4), 531-540. <https://doi.org/10.1161/CIRCRESAHA.108.188524>
- 21 Wei, J., Song, J., Jiang, S., Zhang, G., Wheeler, D., Zhang, J., . . . Liu, R. (2017). Role of intratubular
22 pressure during the ischemic phase in acute kidney injury. *Am J Physiol Renal Physiol*,
23 312(6), F1158-F1165. <https://doi.org/10.1152/ajprenal.00527.2016>
- 24 Wendel, M., Knels, L., Kummer, W., & Koch, T. (2006). Distribution of endothelin receptor subtypes
25 ETA and ETB in the rat kidney. *J Histochem Cytochem*, 54(11), 1193-1203.
26 <https://doi.org/10.1369/jhc.5A6888.2006>

- 1 Wilhelm, S. M., Simonson, M. S., Robinson, A. V., Stowe, N. T., & Schulak, J. A. (1999). Endothelin
2 up-regulation and localization following renal ischemia and reperfusion. *Kidney Int*, 55(3),
3 1011-1018. <https://doi.org/10.1046/j.1523-1755.1999.0550031011.x>
- 4 Yamamoto, T., Tada, T., Brodsky, S. V., Tanaka, H., Noiri, E., Kajiya, F., & Goligorsky, M. S.
5 (2002). Intravital videomicroscopy of peritubular capillaries in renal ischemia. *Am J Physiol*
6 *Renal Physiol*, 282(6), F1150-1155. <https://doi.org/10.1152/ajprenal.00310.2001>
- 7 Yamamoto, Y., Ikegaki, I., Sasaki, Y., & Uchida, T. (2000). The protein kinase inhibitor fasudil
8 protects against ischemic myocardial injury induced by endothelin-1 in the rabbit. *J*
9 *Cardiovasc Pharmacol*, 35(2), 203-211. <https://doi.org/10.1097/00005344-200002000-00005>
- 10 Yamasawa, H., Shimizu, S., Inoue, T., Takaoka, M., & Matsumura, Y. (2005). Endothelial nitric
11 oxide contributes to the renal protective effects of ischemic preconditioning. *J Pharmacol Exp*
12 *Ther*, 312(1), 153-159. <https://doi.org/10.1124/jpet.104.074427>
- 13 Yemisci, M., Gursoy-Ozdemir, Y., Vural, A., Can, A., Topalkara, K., & Dalkara, T. (2009). Pericyte
14 contraction induced by oxidative-nitrative stress impairs capillary reflow despite successful
15 opening of an occluded cerebral artery. *Nat Med*, 15(9), 1031-1037.
16 <https://doi.org/10.1038/nm.2022>
- 17 Ysebaert, D. K., De Greef, K. E., Vercauteren, S. R., Ghielli, M., Verpooten, G. A., Eyskens, E. J., &
18 De Broe, M. E. (2000). Identification and kinetics of leukocytes after severe
19 ischaemia/reperfusion renal injury. *Nephrol Dial Transplant*, 15(10), 1562-1574.
20 <https://doi.org/10.1093/ndt/15.10.1562>
- 21 Zhang, Z., Payne, K., & Pallone, T. L. (2018). Adaptive responses of rat descending vasa recta to
22 ischemia. *Am J Physiol Renal Physiol*, 314(3), F373-f380.
23 <https://doi.org/10.1152/ajprenal.00062.2017>
- 24 Zhang, Z., Rhinehart, K., Kwon, W., Weinman, E., & Pallone, T. L. (2004). ANG II signaling in vasa
25 recta pericytes by PKC and reactive oxygen species. *Am J Physiol Heart Circ Physiol*, 287(2),
26 H773-781. <https://doi.org/10.1152/ajpheart.01135.2003>

27

1 Figures and legends



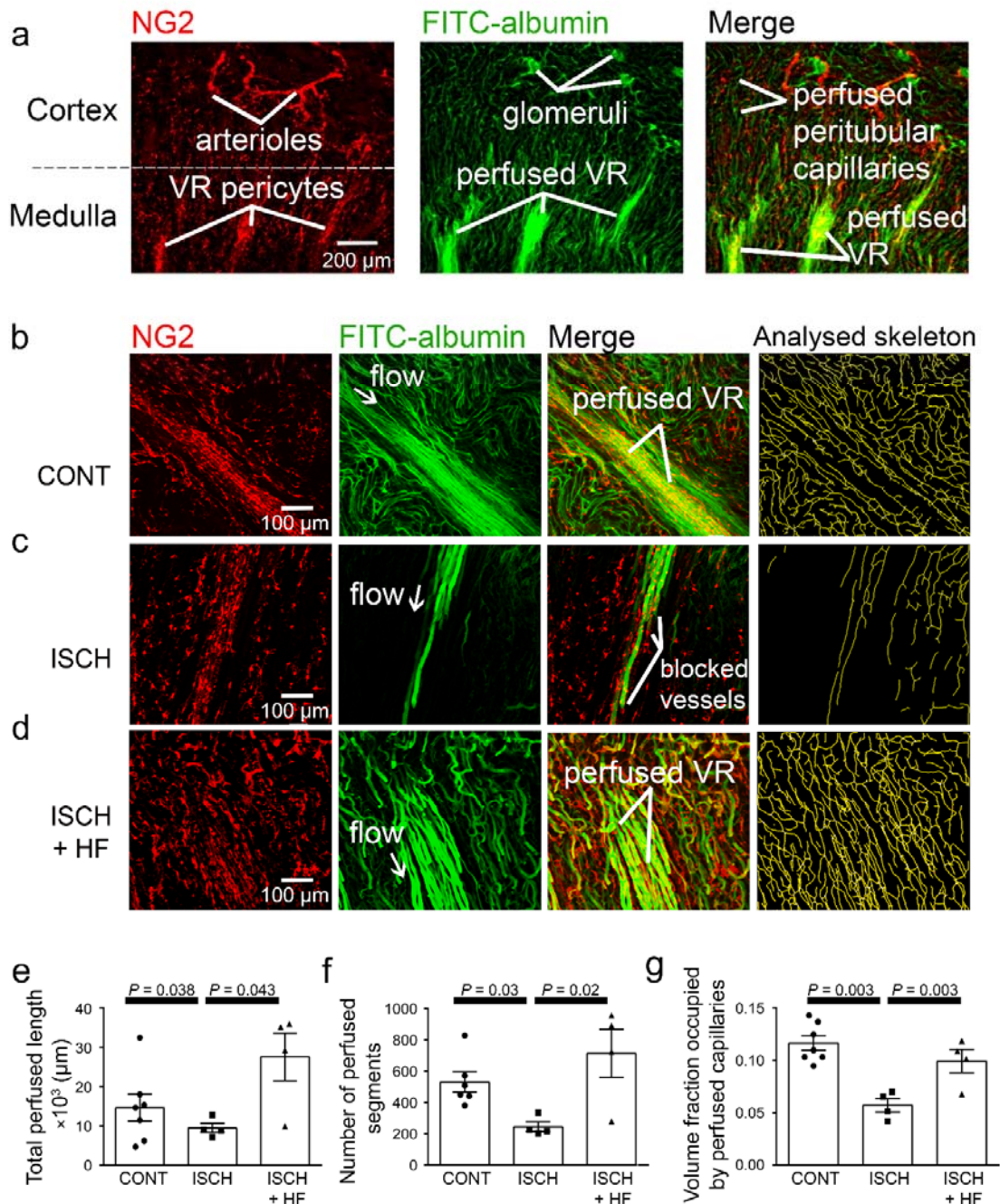
2

3 **Figure 1: Ischemia and reperfusion lead to cortical and medullary no-reflow.**

4 **(a, b)** Ischemia (ISCH) evoked changes of blood flow (measured by laser Doppler) in the rat renal **(a)**
5 medulla (n=4 animals) and **(b)** cortex (n=10 animals). CONT indicates blood flow on the contralateral
6 (non-ischemic) side. Traces labeled +HF show the effect on recovery of perfusion of administering
7 the Rho kinase inhibitor hydroxyfasudil (HF) immediately on reperfusion (ISCH+HF) (n=4 animals).
8 **(c-e) Top:** low power views of kidney slices after perfusion *in vivo* with FITC-albumin gelatin, from

1 (c) control (contralateral) kidney, (d) a kidney after ischemia and 30 min reperfusion, and (e) a kidney
2 30 mins after treatment with HF on reperfusion **Bottom:** regions of interest (ROIs) are shown in red
3 and blue for the cortex and medulla. (f) Medullary perfusion (assessed in slices of fixed kidney as the
4 total intensity of FITC-albumin summed over the ROIs) was reduced after 30 mins of post-ischemic
5 reperfusion (51 stacks, 6 animals) by ~50% compared with control kidneys (52 stacks, 7 animals).
6 Treatment with HF increased medullary perfusion 2.3-fold at this time compared with non-treated
7 ischemic kidneys (20 stacks, 4 animals). (g) Cortex perfusion (assessed as in c-e) after 30 mins of
8 reperfusion after ischemia was reduced by ~23.5% compared with control kidneys. Treatment with
9 HF (ISCH+HF) increased cortex perfusion by 25% at this time compared with non-treated ischemic
10 kidneys (ISCH). Data are mean±s.e.m. *P* values are corrected for multiple comparisons. Statistical
11 tests used the number of animals as the N value.

12



1

2 **Figure 2: Ischemia and reperfusion reduce medullary microvascular perfusion.**

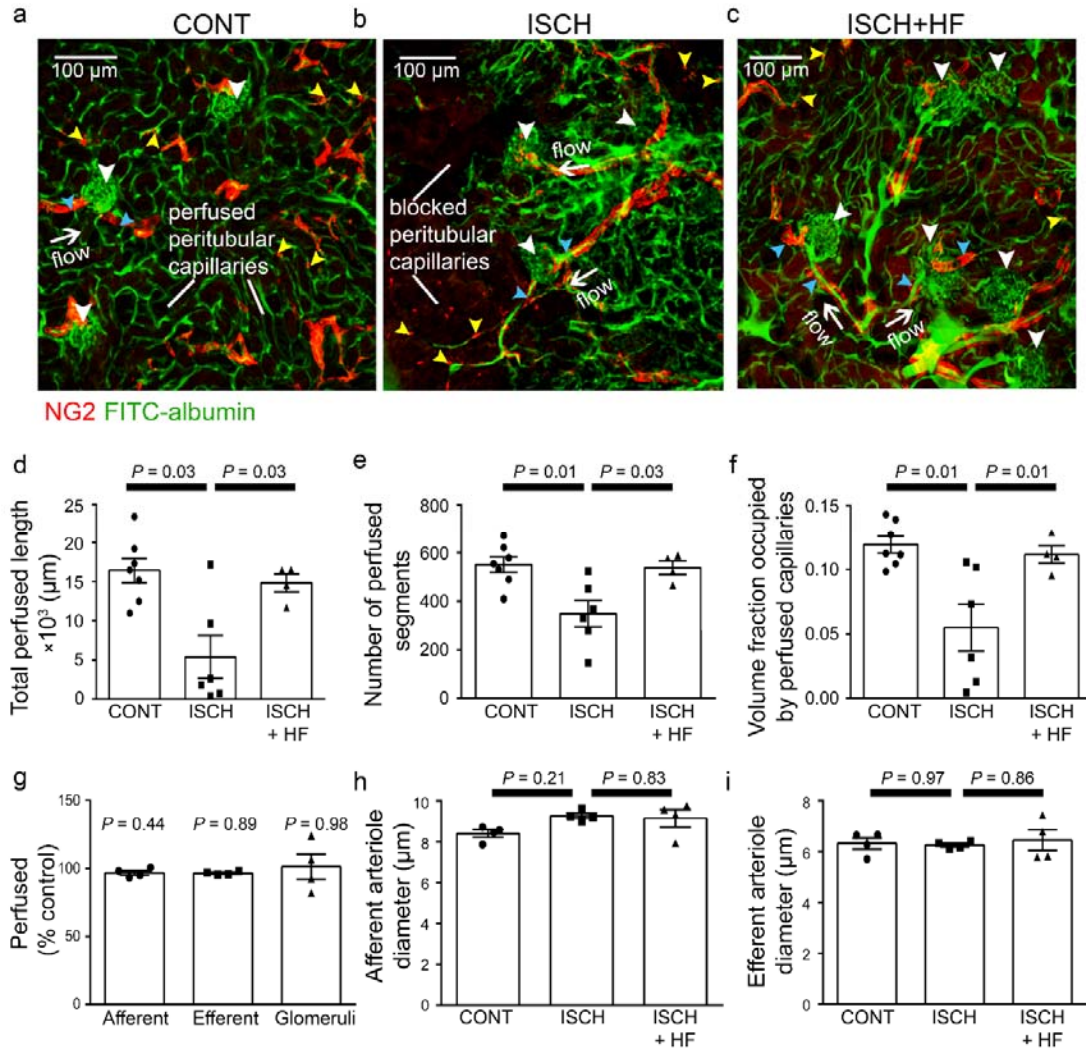
3 (a) Representative images of slices after perfusion with FITC-albumin gelatin, showing the rat kidney

4 microcirculation in 100 μm deep confocal z-stacks. Images depict renal cortical arterioles, the

5 glomeruli and peritubular capillaries, as well as the vasa recta capillaries (VR) that supply blood to the

6 renal medulla. (b-d) Representative images of the medullary microcirculation: (b) in control

1 conditions, **(c)** after ischemia and 30 mins reperfusion, and **(d)** after ischemia and reperfusion for 30
2 mins with hydroxyfasudil (HF) applied during reperfusion (ISCH+HF). Images show NG2-labelling
3 of pericytes (red), FITC-albumin labelling (green) of vessels that are perfused, a merge of the NG2
4 and FITC-albumin images, and the analysed skeleton (yellow) of the perfused microvessels. **(e-g)**
5 After ischemia and reperfusion (12 stacks, 4 animals), the total perfused capillary length **(e)**, the
6 number of perfused capillary segments **(f)** and the overall volume fraction of vessels perfused **(g)** in
7 100 μm deep confocal z-stacks were reduced compared with control kidneys (14 stacks, 6-7 animals),
8 and treatment with hydroxyfasudil immediately after reperfusion (10 stacks, 4 animals) increased all
9 of these parameters. Data are mean \pm s.e.m. *P* values are corrected for multiple comparisons. Statistical
10 tests used the number of animals as the N value.

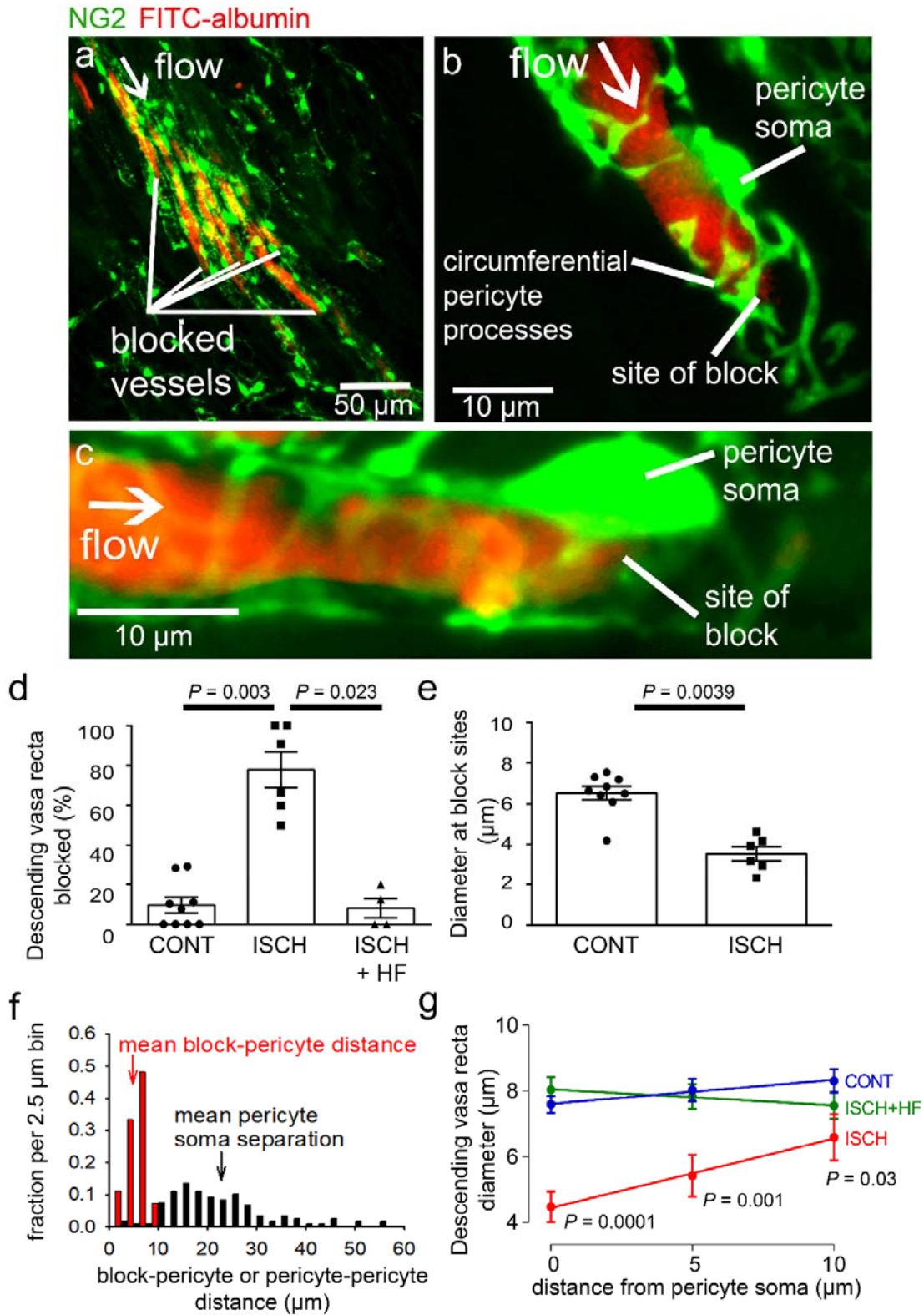


1

2 **Figure 3: Ischemia and reperfusion of renal cortex evoke no-reflow in capillaries but not**
3 **arterioles.**

4 (a-c) Representative images of rat renal cortex slices containing arterioles, glomeruli and peritubular
5 capillaries, after perfusion with FITC-albumin gelatin: (a) for control kidneys (CONT), (b) after
6 ischemia and reperfusion (ISCH), and (c) after ischemia with hydroxyfasudil (ISCH+HF). NG2-
7 labelling is seen of arterioles and pericytes (red) (yellow arrowheads), while FITC-albumin labelling
8 (green) shows vessels that are perfused. (d-f) After ischemia and reperfusion (12 stacks, 6 animals),
9 the total perfused capillary length (d), the number of perfused segments (e), and the overall perfused
10 microvascular volume fraction (f) were reduced compared with control kidneys (14 stacks, 7 animals),
11 and treatment with hydroxyfasudil immediately after reperfusion (10 stacks, 4 animals) increased

1 cortical microvascular perfusion compared with non-treated ischemic kidneys. **(g)** Percentage of
2 afferent and efferent arterioles (blue arrowheads in a-c), and of glomeruli (white arrowheads),
3 perfused after ischemia, compared with control conditions. **(h-i)** Diameters of perfused **(h)** afferent
4 and **(i)** efferent arterioles in the renal cortex for the three experimental conditions (15 arterioles, 4
5 animals for each group). Data are mean±s.e.m. *P* values are corrected for multiple comparisons.
6 Statistical tests used the number of animals as the N value.
7

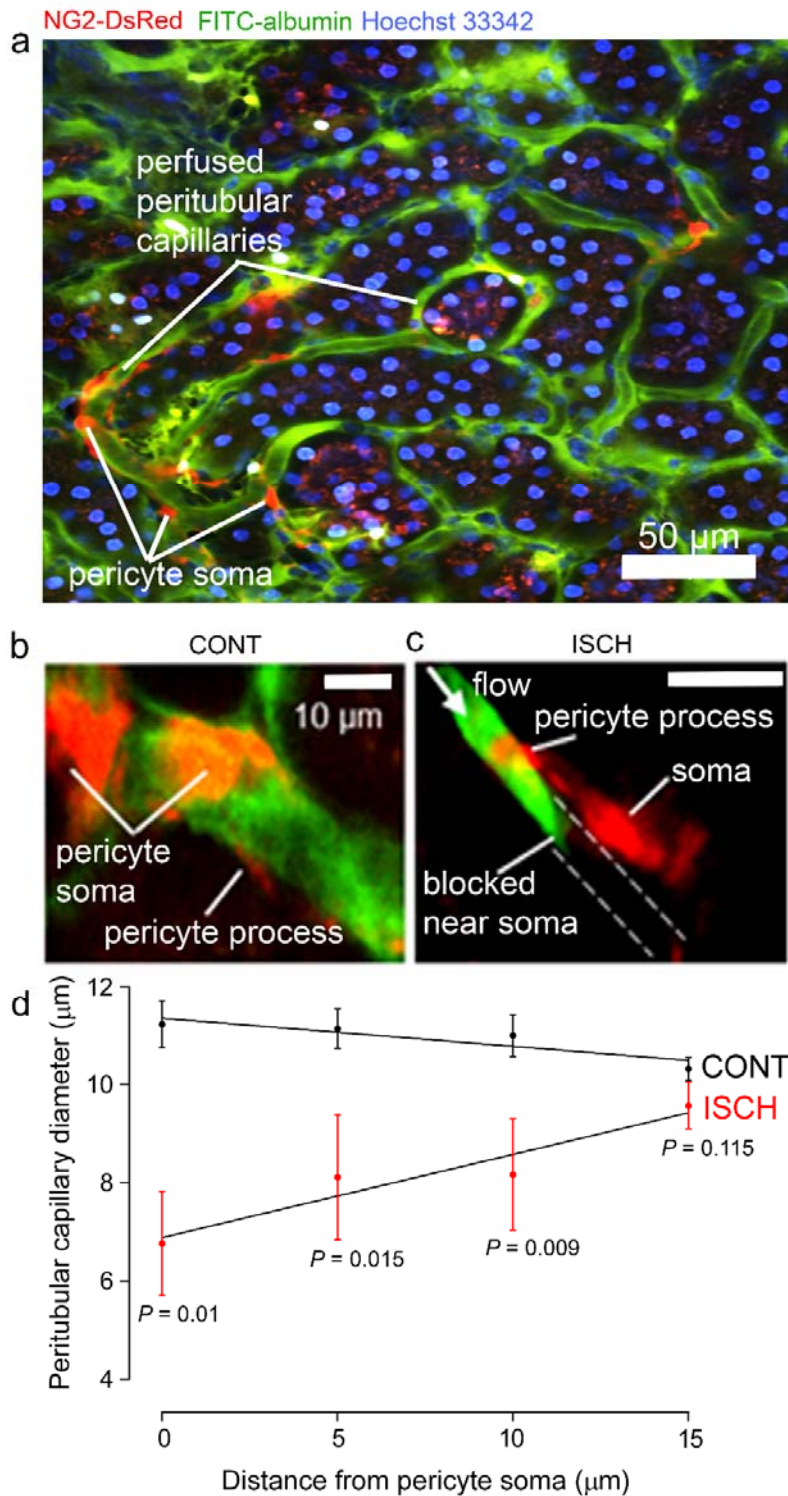


1

2 **Figure 4: Descending vasa recta are constricted by pericytes after ischemia.**

1 (a) Descending vasa recta (DVR) in slices of rat renal medulla after perfusion with FITC-albumin
2 gelatin (re-coloured red), and labelled for pericytes with antibody to the proteoglycan NG2 (green);
3 FITC-albumin labeling shows perfused and blocked vessels. White arrow indicates flow direction;
4 white lines indicate blocked vessels. (b-c) Representative images showing DVR capillaries blocked
5 near pericyte somata. NG2-labelling of pericytes shows pericyte processes presumed to be
6 constricting vessels at block site. (d) Percentage of DVR capillaries blocked in the renal medulla in
7 control conditions (127 capillaries, 12 stacks, 9 animals), after ischemia and reperfusion (77
8 capillaries, 10 stacks, 6 animals), and after ischemia with hydroxyfasudil present in the reperfusion
9 period (60 capillaries, 8 stacks, 4 animals). Statistical tests used number of animals as the N value. (e)
10 Diameter at block sites. (f) Probability distribution per 2.5 μm bin of distance from blockage to
11 nearest pericyte soma after ischemia and reperfusion (for 27 block sites), and of the distance between
12 adjacent pericytes on DVR capillaries (for 118 pericyte pairs). (g) DVR diameter versus distance from
13 pericyte somata (10 μm is approximately half the separation between pericytes) in the same 3
14 conditions as d (number of pericytes was 31, 20 and 17 respectively). *P* values by each point are from
15 t-tests. Slope of the best-fit ISCH regression line is significantly greater than zero ($P=0.039$) while
16 that of the CONT line is not ($P=0.084$). Data are mean \pm s.e.m.

17



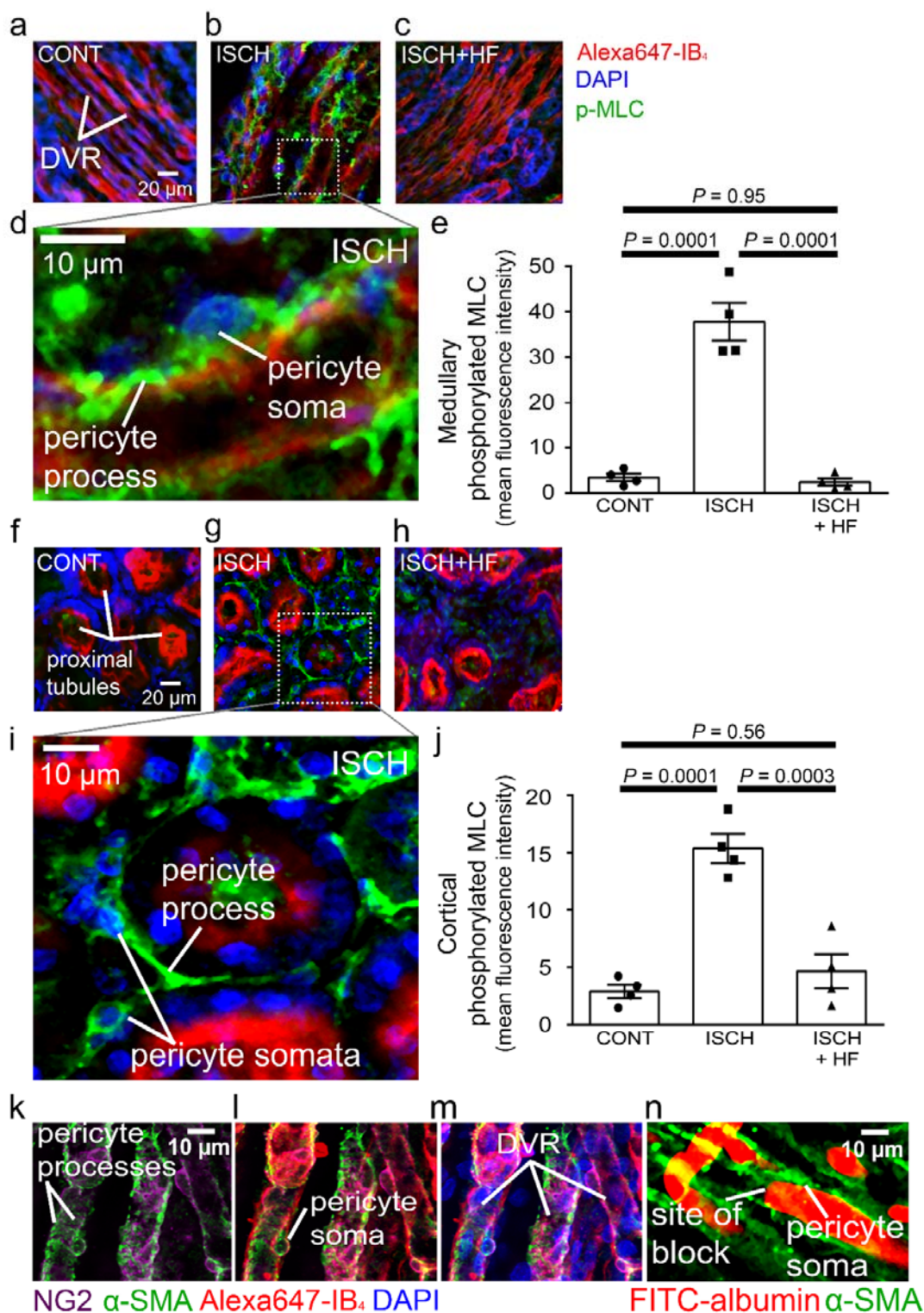
1

2 **Figure 5: Pericytes constrict capillaries after renal ischemia *in vivo*.**

3 (a) Overview 2-photon *in vivo* imaging stack of the mouse renal cortex microcirculation, showing

4 pericytes expressing NG2-DsRed (red), intraluminal FITC-albumin given intravenously (green), and

1 Hoechst 33342 labelling nuclei (blue). Images were acquired in a plane parallel to the cortical surface.
2 **(b, c)** Higher magnification images showing a pericyte on a cortical peritubular capillary in control
3 conditions, and post-ischemic capillary block (dashed lines show path of blocked vessel). **(d)**
4 Capillary diameter versus distance from pericyte somata after ischemia and reperfusion (ISCH), and
5 for control kidneys (CONT) (number of pericytes was 15 and 10 respectively from 10 stacks from 3
6 animals from each group). Slope of the best-fit ISCH regression line is significantly greater than zero
7 ($P=0.046$) while that of the CONT line is negative but not significantly different from zero ($P = 0.10$).
8 Data are mean \pm s.e.m. P values comparing data at each distance are corrected for multiple
9 comparisons. Statistical tests used number of images as the N value.
10

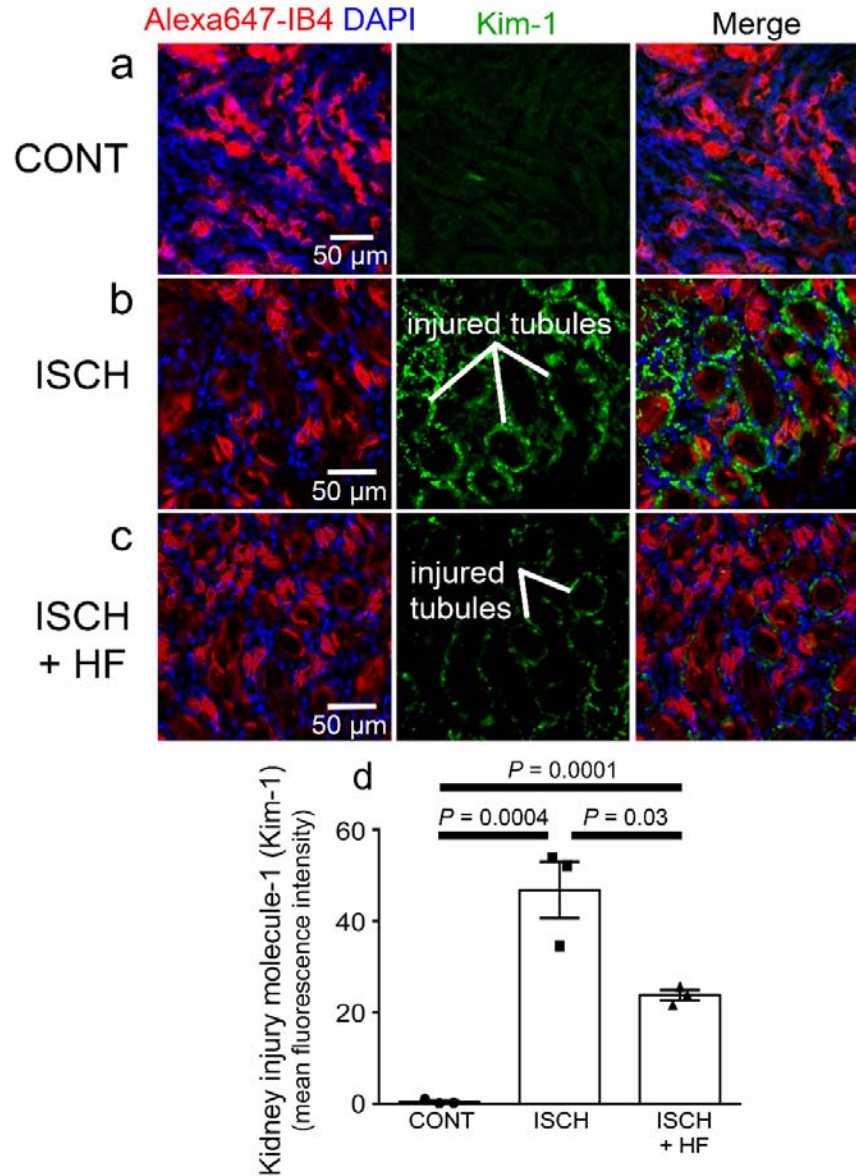


1

2 **Figure 6: Pericyte contraction is mediated by α -SMA and regulated by Rho kinase.**

1 Representative images of the rat renal medulla containing descending vasa recta (DVR) pericytes (**a-**
2 **d**) and cortical peritubular capillary pericytes (**f-i**), labelled with antibody to phosphorylated myosin
3 light chain (p-MLC, green), Alexa Fluor 647-isolectin B₄ which labels kidney tubules and pericytes
4 (red), and DAPI which labels nuclei (blue). Labelling is shown for kidneys in control conditions
5 (CONT) (**a, f**), after ischemia and reperfusion (ISCH) (**b, d, g, i**), and after ischemia with
6 hydroxyfasudil present during reperfusion (ISCH+HF) (**c, h**). (**e, j**) Cortical (**e**) and medullary (**j**) p-
7 MLC levels in pericytes for the three experimental conditions (10 stacks, 4 animals for each group,
8 statistical tests used the numbers of animals for N values). (**k-m**) DVR pericytes labelled for NG2
9 (purple), α -SMA (green), Alexa647-isolectin B₄ (red) and DAPI (blue). (**n**) DVR blockage-associated
10 pericyte labelled for α -SMA. Data are mean \pm s.e.m. *P* values are corrected for multiple comparisons.

11

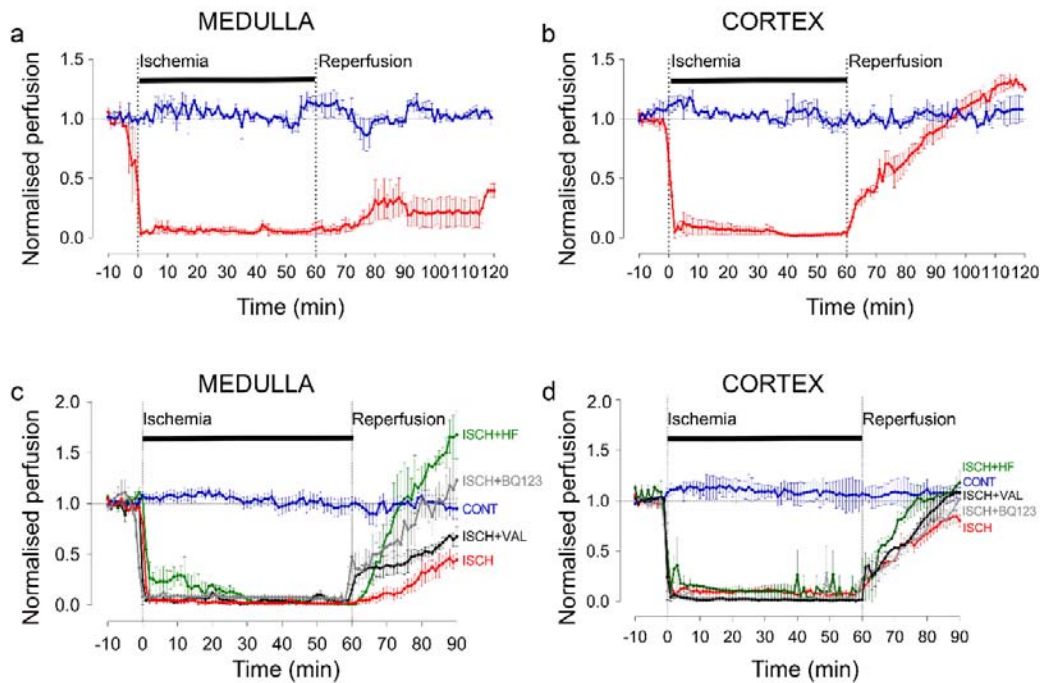


1

2 **Figure 7: Rho kinase inhibition reduces kidney injury induced by ischemia and reperfusion.**

3 (a-c) Images of the rat renal cortex containing proximal tubules, showing isolectin B₄ labelling kidney
4 tubules (red), DAPI labelling nuclei (blue), and kidney injury molecule-1 (Kim-1) labelling as an
5 injury marker (white lines indicate examples of injured tubules labelled in green), for control
6 conditions (CONT) (a), after ischemia and reperfusion (ISCH) (b), and after ischemia with
7 hydroxyfasudil present during reperfusion (ISCH+HF) (c). (d) Kim-1 levels for the three experimental

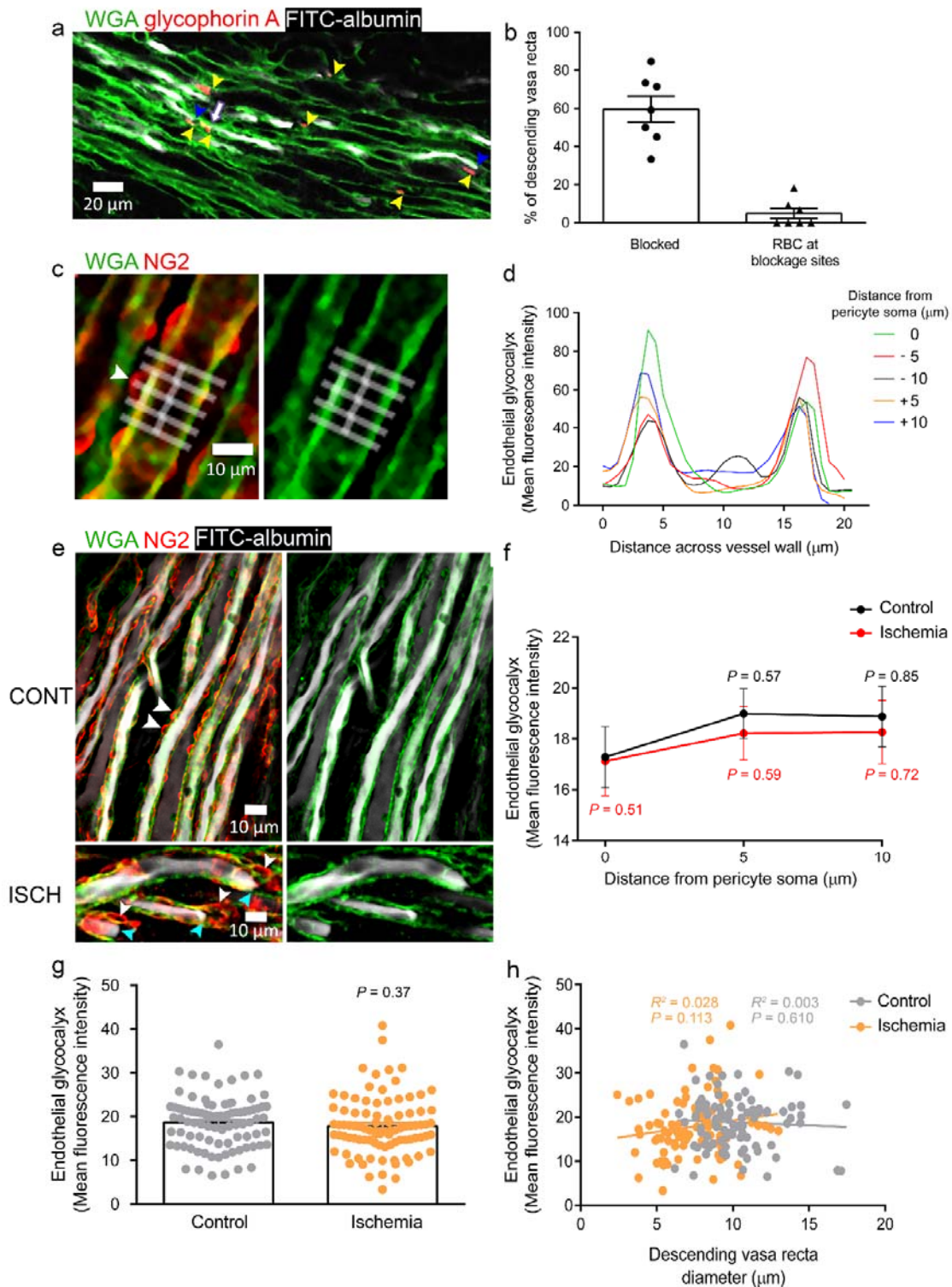
- 1 conditions (6 stacks, 3 animals for each group). Data are mean \pm s.e.m. *P* values are corrected for
- 2 multiple comparisons. Statistical tests used the number of animals as the N value.
- 3



1

2 **Figure S1:** (a, b) Ischemia (ISCH) evoked changes of blood flow (measured by laser Doppler) in the
3 rat renal (a) medulla (n=3 animals) and (b) cortex (n=3 animals). CONT indicates blood flow on the
4 contralateral (non-ischemic) side. At 60 min following reperfusion, medullary perfusion remained
5 compromised at 40% of its control value ($P=0.017$), but cortical perfusion was fully recovered (to
6 ~20% above the control value, although this did not reach significance, $P=0.092$). (c)
7 Hydroxyfasudil (3 mg/kg; i.v.) treatment immediately after reperfusion (ISCH+HF) induced a faster
8 recovery to the pre-ischemic value of of medullary blood flow than did BQ123 (0.5 mg/kg, i.v.,
9 given on reperfusion: ISCH+BQ123), a selective endothelin-A receptor antagonist. After 30 min
10 reperfusion both agents resulted in blood flow that was not significantly different from control
11 ($P=0.8$ and $P=0.38$, respectively) but was significantly different from ischemia ($P=0.01$ for both
12 drugs). Valsartan (1 mg/kg i.v., given on reperfusion: ISCH+VAL), an angiotensin II type 1 (AT1)
13 receptor antagonist, increased medullary perfusion by 52% after 30 mins reperfusion compared with
14 non-treated ischemic kidneys, although this did not reach significance ($P=0.11$ vs. ISCH) and
15 valsartan had not reversed medullary blood flow to the baseline level after 30 mins ($P= 0.19$ vs.
16 CONT). (d) Recovery of cortical blood flow to its control level on reperfusion was faster in the

- 1 presence of hydroxyfasudil (ISCH+HF). BQ123 ($P=0.05$ vs. ISCH) and valsartan ($P=0.04$ vs. ISCH)
- 2 also promoted recovery of cortical blood flow at 30 min reperfusion compared with non-treated
- 3 ischemic kidneys (ISCH). Statistical tests used the number of animals as the N value.
- 4
- 5



1

2 **Figure S2:** (a) Red blood cells (RBCs, indicated by yellow arrowheads, labelled for glycophorin A)
 3 were associated with a small percentage of blockage sites (indicated by blue arrowheads) in ischemic
 4 rat kidneys (5.8% of 85 blockages from 137 vessels analysed from 2 animals), and even where red

1 blood cells were near the capillary blockages it did not always lead to a block of blood flow (as
2 shown by FITC-albumin, re-coloured white, passing the red blood cells [purple arrow]). Note that
3 the vasculature was perfused with PBS to remove loose RBCs before perfusing PFA and FITC-
4 albumin, so the only RBCs remaining should be those bound to the vessel walls. **(b)** Percentage of
5 DVR that were blocked, and percentage of blocked DVR that had an associated RBC. **(c)** Endothelial
6 glycocalyx (eGCX) was labelled in vivo using wheat germ agglutinin-Alexa Fluor 647 (WGA, re-
7 coloured green). White boxes show ROIs for measuring eGCX mean fluorescence intensities at
8 different distances from the pericyte soma. **(d)** Plots of WGA signal across capillary at different
9 distances from arrowed pericyte in (c). **(e)** eGCX is fairly evenly distributed along the vessel wall in
10 normal kidneys, and also after ischemia and reperfusion. Blockages (indicated by blue arrowheads)
11 are highly associated with pericyte location (indicated by white arrowheads) in ischemic kidneys
12 (ISCH). **(f)** Mean level of eGCX averaged across vessel at different distances from the pericyte soma
13 in control kidney and after ischemia with 30 mins reperfusion. For the control condition, black *P*
14 values compare the value at each position with that at the soma. Red *P* values compare the ischemic
15 and control groups for each position). **(g)** eGCX mean fluorescence averaged over all positions
16 measured. **(h)** eGCX intensity and diameter have no correlation in control or ischemic conditions.
17 Data are mean±s.e.m, 30 pericytes from 2 animals for each experimental condition. Statistical tests
18 used the number of pericytes as the N value.
19